UNIVERSITÀ DEGLI STUDI DI PADOVA

DIPARTIMENTO DI BIOLOGIA

Corso di Laurea in Biologia Molecolare

ELABORATO DI LAUREA

Circular RNA ANAPC7 Inhibits Tumor Growth and Muscle Wasting via PHLPP2–AKT–TGF-b Signaling Axis in Pancreatic Cancer

Tutor: Prof. Marco Sandri
Dipartimento di Scienze Biomediche
Sede: V.I.M.M.-Veneto Institute of Molecular Medicine

Laureando: Samuele Graziano

ANNO ACCADEMICO 2023/2024

Per Mario e tutta la sua famiglia,
che questo sia il mio primo passo per,
nel mio piccolo,
combattere questa malattia.
Sarete sempre nei miei pensieri.

INDEX

ABSTRACT

Pancreatic cancer is the cancer-type inducing the most severe cachectic phenotype. Recent studies describe ZIP4 as a main factor inducing pancreatic cancer through oncogenic miR-373 up regulation. The purpose of this study is to identify circular RNAs (circRNAs) able to mitigate the oncogenic activity of the ZIP4/miR-373 pathway. This study reveals circANAPC7 as a novel tumor suppressor, capable of buffering miR-373 molecules with a consequent increase of PHPLPP2 phosphatase activity. Accordingly, AKT/STAT5 pathway is downregulated such as the release of muscle wasting molecule TGF- β. In my thesis, I am describing this recent scientific manuscript, recently published, deeply discussing the scientific questions driving this work and the techniques applied to solve them.

INTRODUCTION

Pancreas generalities

Pancreas is a glandular organ located in the upper abdominal area, behind the stomach, and could reach 15 cm in length and 70/80 g in weight. This organ presents both endocrine function, essential for blood sugar level regulation thanks to regulative hormones secretion into blood stream (i.e. insulin, glucagon and somatostatin); and exocrine function involved in stomach pH regulation and digestive enzymes secretion into digestive duct. From an anatomical point of view, it can be divided into three parts: the head, which is held stable by the duodenum; the body, and the tail. More than 80% of the organ mass is made of lobular structures formed by the cells responsible for hormones or enzymes secretion. Lobules of exocrine pancreas are interconnected by ducts, which allow to the secreted "pancreatic juice" to flow into the pancreatic duct, which runs from the tail to the head, pouring into the duodenum via the greater papilla. The digestive enzymes, released inside the pancreatic juice, lead to macronutrients degradations: fats, carbohydrates, proteins and nucleic acids. Many are synthesized as pro-enzymes (e.g. trypsinogen, chymotrypsinogen, etc.) and then activated in the desired digestive district to prevent undesired catalytic activity, that can lead to tissue damage [(1)]. Histologically, endocrine pancreas cells constitute clusters called Langerhans islets, dispersed among exocrine pancreas cells that represent most of this organ cell type. Actually, 5 different cell type has been identified inside each Langerhans islet:

- α cells: produce glucagon responsible for raising glycemia;
- β cells: release insulin responsible for reducing glycemia;
- γ cells: produce the pancreatic polypeptide that reduces the intestinal contraction;
- δ cells: release somatostatin responsible for the inhibition of GH hormone;
- ε cells: produce ghrelin that induces hunger.

Malfunctioning or dysregulation of both endocrine and/or exocrine activities can lead to serious pathologies. An example is represented by T2DM and T1DM, where

blood sugar levels are out of control, compromising the physiology of all other organs and needing an urgent therapeutical approach. Even worse is a pancreatic cancer scenario in which both exocrine and endocrine activities are irreversibly damaged, with a minimum spectrum of therapeutical intervention.

Pancreatic cancer: a brief insight

Pancreatic cancer presents a high mortality rate. Only 10% of patients survive beyond 5 years from the prognosis when the tumor is metastatic. This number increases to 20% in patients with a localized and operable tumor (5 years post-surgery). Several studies have shown that the incidence rate is growing so much that it has become one of the leading causes of death in the world. There are many factors that could promote the development of this cancer, both genetics and environmental, such as: obesity since pancreatic intraepithelial fat promotes the development of cancer cells precursor. Moreover, as many other cancer typology, low-quality lifestyle represented by alcohol consumption, poor nutrition and smoking represent an additive risk factor. From genetic point of view, only 5-10% of total pancreatic cancer cases can be attributed to hereditary factors as oncogenes alteration: *STK11* (p[1]>35%), *SPINK1* and *PRSS1* (p>40%) associated to chronic pancreatitis. Pancreatic cancer could essentially be divided into 2 categories: ductal adenocarcinoma, which concerns the exocrine part of the organ, and neuroendocrine tumors which are much less frequent. In particular, neuro endocrine tumors can originate from all the cells belonging to Langerhans islets, for this reason, it can generate several different types of cancer with different symptoms [(2)].

One of the main factors that makes the life expectancy of a patient with pancreatic cancer so low is due to the systemic importance of this organ and its central role in metabolic and glycemic homeostasis, furthermore, it is not giving strong symptoms in first stages of the disease. In addition, cancer has a very high correlation with the onset of cachexia, a further factor that reduces the prognosis.

[1] p = probability to develop cancer.

Pancreatic tumor and cachexia

Cachexia is a multifactorial syndrome that induces sarcopenia, adipopenia and, in general, a reduction in hunger and available energy. Cachexia could be the consequence of many diseases, including cancer; precisely, about 50% of cancer patients rising to 80% in pancreatic cancer patients. Cachexia systemic effects decrease patients' life expectation mainly because a lower living standards and poor pharmacological therapies effects. For these reasons, approximately 33% of pancreatic cancer deaths can be related to cachexia.

Cancer cachexia hyper-catabolic state is mainly due to the systemic inflammatory response caused by tumor induced metabolic alterations, which promotes adipose tissue and skeletal muscle loss. Furthermore, tumor-derived chronic inflammatory condition is well characterized by the increasing levels of circulating cytokines, such as IL-6 and TGF- β [(3)].

Research conducted on preclinical models has revealed a correlation between muscle loss and survival of animals with tumors. This means that reversing cachexia, the condition associated with muscle wasting, leads to tangible survival benefits, regardless of tumor progression [(4)].

ZIP4 and TGFβ role in tumor growth and cancer cachexia

IL-6 is a pro-inflammatory cytokine chronically overexpressed in several pathological conditions. Its overexpression from pancreatic cancer cells facilitates both tumor growth and immune surveillance evasion. For example, IL-6 dependent STAT3 activation triggers a higher production of Cyclin D1, an important cell growth factor.

In recent studies, the authors of the scientific paper discussed here understood that the increased production of IL-6 can be mediated by the overexpression of ZIP4. ZIP4 is a transmembrane zinc ion transporter protein; it is essential for the activation of many transcription factors containing zinc finger motifs, including CREB. The latter is one of the main actors in IL-6 transcriptional up-regulation. [(5)].

In the following article, it will be shown and discussed how ZIP4 is responsible of both IL-6 and TGF- β overexpression. TGF-β is a pleiotropic cytokine involved in

cachexia. It is a Smad-related pathway activator. Smad3 mediates the oxidation and nitrosylation of ryanodine receptor 1 (RyR1), which in turns reduces the presence of this $Ca2^{+}$ channel in the sarcoplasmic reticulum causing muscle weakness. Moreover, Smad3 induces Nox4 gene transcription increasing ROS production and a pro-oxidative cellular state as consequence [(6)]. Remarkably, Smad2-3 complex activation induces the proteolytic ubiquitin-proteasome signaling pathway, a process deeply studied in skeletal muscle tissue leading to muscle atrophy, a cornerstone process involved in cachexia. To note, Smad2/3 complex inhibits the myogenic pathway mediated by the Akt/mTOR axis [(7)]. Recently, different studies have been conducted to target specific members of the just described signaling pathways. Besides "classic" pharmacological interventions, increasing attention is addressed to the role of circular RNAs and how they can be exploited to treat or mitigate tumor growth and cancer cachexia.

Circular RNAs and their role in cancer

CircRNA is a type of ncRNA whose structure comprises covalently closed loops with no polyadenylated tails at the 3' ends or cap structure at the 5' ends. Thanks to this construction, circRNAs can avoid exonuclease degradation and have a longer half-life than their parental mRNAs (48 hours vs 10 hours) [(8)]. The study of circRNAs has increased exponentially in recent years since their fundamental role in cellular metabolic regulation has been discovered. Its role is so important that their dysregulation can induce various pathologies including cancer. They can regulate the expression of parental genes at the epigenetic level, modulate alternative splicing, regulate RNA-protein interactions, act as scaffolds in the assembly of protein complexes and regulates miRNA activity [(9)]. CircRNAs can be good biomarkers for cancer diagnosis and prognosis or therapeutic agents to inhibit oncogenic microRNAs or proteins. In fact, circRNAs located in the cytoplasm can participate in post-transcriptional gene regulation through miRNA sponging, thus preventing specific oncogenic miRNAs from interacting and repressing their potential target mRNAs. At the same time, circRNAs that induce tumors can be selectively inhibited or degraded using antisense technology. Novel cancer

therapies could also rely on the acquisition of circRNA function, either through the overexpression of natural tumor suppressor circRNAs or through the expression of artificial circRNAs that contain tumor suppressor elements [10]. In the article that I am going to describe, we will discuss about circRNA ANAPC7 and its specific role in pancreas cancer induced cachexia.

METHODS AND RESULTS

The experimental core of this work was to further investigate the ZIP4-miR-373 pathway, being already aware that this molecular axis is correlated to pancreatic tumor progression. The purpose of the study was to identify a possible regulative role of circular RNAs on ZIP4-miR-373 pathway.

During these studies, different pancreatic tumor cell lines has been used as model, especially because this kind of *in vitro* models represent a gold standard for tumor related signaling pathways studies. In particular, the most used cell lines were:

- AsPC-1, a **pro-cachectic** line that derived from ascites;
- MIA PaCa-2, a **non-cachectic** line that derives from epithelium.

Moreover, further experiments have been conducted on more "complex" models as, for example, 3-dimensional spheroid and organoid cultures. Finally, during last study stage they evaluated tumor progression from both molecular and physiological point of view on orthotopic xenografts mouse models.

Discovery and function of circANAPC7

First of all, Min Li and his team worked at bioinformatics level to find out which circRNAs, with specific miR-373 binding sites, had different expression level in pancreatic tumor and adjacent tissues compared to the healthy ones. Among the down-regulated circRNAs, they decided to focus on circANAPC7 after observing its enrichment through RT-qPCR performed on a biotinylated miRNA Pulldown assay using miR-373 as bait (fig.1).

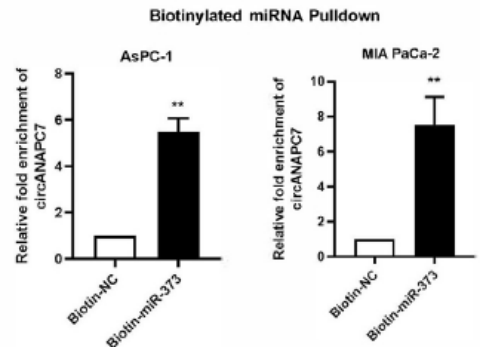

Figure 1: circANAPC7 level enrichment using miR-373 as bait on a Biotinylated miRNA Pulldown.

At this point, to understand if circANAPC7 acts on miR-373 individually or if it acts through a protein scaffold, an RNA-Immuno Precipitation was performed, using circANAPC7 as bait. They obtained an enrichment of AGO2, a well-known protein complex essential for the processing of miRNA degradation. The authors concluded that circANAPC7 work as molecular mediator for AGO2-mediated miR-373 degradation.

Considering that circANAPC7 expression level is significantly lower in a pancreatic tumor context than in physiological conditions, scientists thought to over-express this circRNA in AsPC-1 and MIA PaCa-2 cells, both in 2D and 3D cultures to understand its possible effects on pancreatic cancer context. Precisely, thanks to EdU assay, colony formation assay and methylcellulose-based 3D cancer cell spheroid images, a drastic reduction of cell proliferation was observed (fig.2). This result led them to think that circANAPC7 was a good study model to contrast pancreatic tumor cell growth. However, at this point of the study, the pro-cancerogenic signaling pathway downstream ZIP4-miR-373 remains elusive. Consequently, researchers decide to focus their attention to the novel discovered circANAPC7, remaining in pancreatic cancer context.

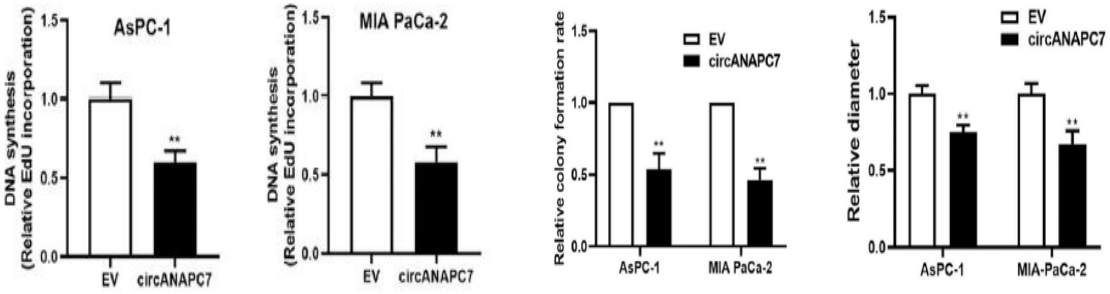

Figure 2: circANAPC7 inhibitory effect on cell proliferation identified through EdU assay, colony formation assay and 3D cell spheroid images.

PHLPP2 role in ZIP4-miR-373 pathway

To understand the main ZIP4-miR-373 pathway member involved in cell proliferation induction, researchers performed analyses on miR-373 downstream targets. They showed that phosphatase PHLPP2 was negatively correlated to miR-373, but positively correlated to circANAPC7 overexpression.

In particular, they searched for human tumor suppressor genes with both miR-373 binding site and ZIP4 negative correlation, finding 3 candidates. Subsequently, they performed RT-qPCR in a circANPC7 overexpression context identifing PHLPP2 as the only upregulated gene among the 3 candidates.

To corroborate these results, they shown that transcriptional and translational conservation of PHLPP2 is obtained once circANAPC7 is overexpressed or by transfecting cells with a synthetic Anti-miR-373. Since the inhibitory activity of circANAPC7 on miR-373, these results proved that it is the "sponge effect" of circANAPC7 to **indirectly** up-regulate PHLPP2 (fig. 3a-b).

Furthermore, to confirm whether miR-373 acts directly on PHLPP2, a biotinylated miRNA Pulldown was performed and, after the observation of an enrichment of PHLPP2, a luciferase reporter assay was performed to understand in which part of the transcript miR-373 acts. It was found that, by mutagenizing the expression vector for PHLPP2-linked luciferase at the PHLPP2 3' UTR level, a greater luciferase activity was obtained. Indicating therefore, a lower incidence of miR-373 on the translation activity in the case of mutation at the 3'UTR, that confirms this as the binding region (fig.3c).

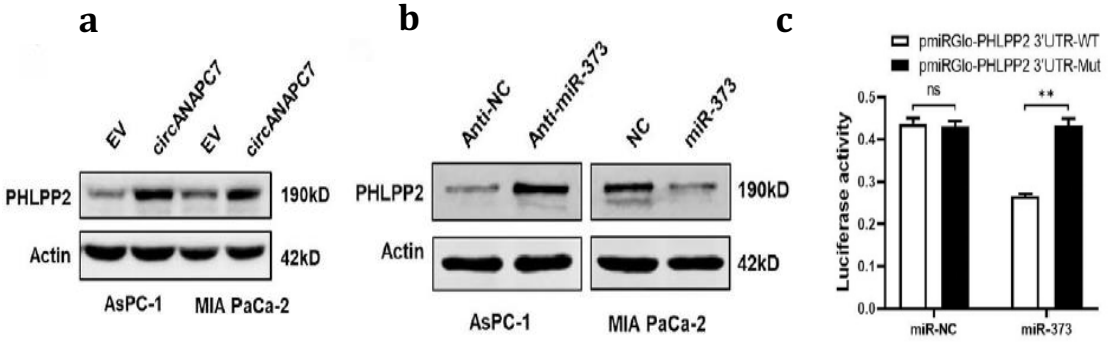

Figure 3: a) Western Blot assay indicates higher PHLPP2 protein expression level when circANAPC7 is overexpressed in different pancreatic cancer cell lines. b) Western Blot assay indicates higher PHLPP2 protein expression level when Anti-miR-373 is overexpressed in different pancreatic cancer cell lines. c) Luciferase activity reports PHLPP2 binding region with miR-373.

PHLPP2 has recently been identified as an inhibitor of the kinase activity of AKT, a protein involved in cell proliferation activity, through its dephosphorylation. For this reason, the following experiment was set up to verify whether AKT phosphorylation levels were affected by miR-373 and circANAPC7 level. Both 2D and 3D cultures were grown, silencing ZIP4 avoiding to activate ZIP4-miR-373-PHLPP2 axis. 4 different experimental overexpression conditions were used:

1. With a Empty Vector (EV) as control[2];
2. With miR-373 coding sequence;
3. With coding sequence for both miR373 and circANAPC7;
4. With coding sequence for both miR373 and mutated circANAPC7.

As shown from the WB in fig.6, overexpression of circANAPC7 inhibits miR-373 activity leading to increased PHLPP2 activity resulting in lower AKT phosphorylation status. These results confirm the hypothesis in which circANAPC7 interferes the downstream ZIP4 related pathway acting on PHLPP2 activity.

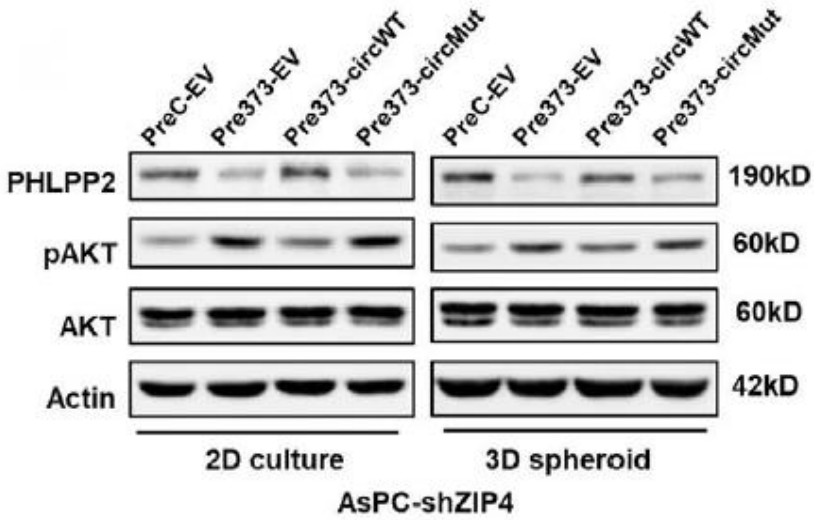

Figure 3: Western Blot (WB) assay indicates higher PHLPP2 protein expression level and lower pAKT protein expression level when circANAPC7 Wild Type is overexpressed, and it indicates lower PHLPP2 protein expression level and higher pAKT protein expression level when circANAPC7 Mutant is overexpressed. WB shows the same results both in 2D colture and 3D spheroid.

[2] The control is necessary to be able to compare different conditions against the unchanged tumor condition/the control itself.

The ZIP4-miR-373-PHLPP2 axis controls tumor proliferation

In previous studies, Li group showed that ZIP4 induces miR-373 transcription through the activity of transcription factor CREB. Since the broad CREB dependent gene regulation network, they wondered if the regulation of PHLPP2 via ZIP4 was due to miR373 exclusively. Comparing two tumor cell lines, one presenting ZIP4 expression suppressed (AsPC-koZIP4) and the other over-expressing ZIP4 (MIA-ZIP4); it was found that PHLPP2 protein levels are higher when ZIP4 is absent or less active (fig.7a). Furthermore, AsPC-shZIP4 line (ZIP4 down-regulated pancreatic tumor cell line) was transfected to induce miR-373 over-expression. As result, they observed a decrease PHLPP2 protein level (fig.7b). Moreover, to further confirm the ZIP4-miR-373-PHLPP2 molecular relations, MIA-ZIP4 cell line (pancreatic tumor cell line with ZIP4 over-expressed) was transfected with a vector expressing miR-373 antagonist obtaining a higher PHLPP2 protein level when compared to respective control (fig.7c).

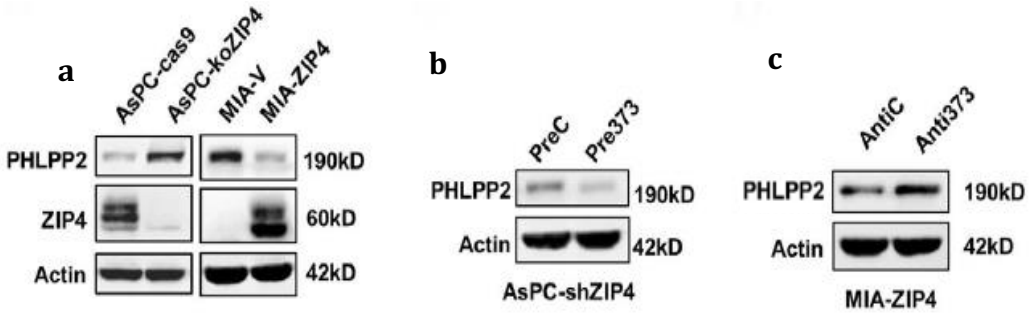

Figure 4: a) Western Blot (WB) assay indicates higher PHLPP2 protein expression level in ZIP4KO cell line.. b) WB assay indicates lower PHLPP2 protein expression level when Pre373 is overexpressed. c) WB assay indicates higher PHLPP2 protein expression level when Anti373 is overexpressed. Actin protein expression level as housekeeping.

Based on these results, Mr. Min Li and collaborators performed multiple mouse xenografts exploiting AsPC-shZIP4-Pre373 cell model, in which ZIP4 is silenced but miR-373 transcription is still present, and MIA-ZIP4-anti373 cell model, where ZIP4 is over-expressed but miR373 is down regulated. Through immunostaining (fig.8) using anti-PHLPP2 and Ki67 antibodies, they reached the same conclusion observed *in vitro*: the presence of miR-373, but not ZIP4, inhibits PHLPP2. On the other hand, while with ZIP4 is still present, but miR-373 is inhibited, PHLPP2 is expressed. In fig.8, we can see also the Ki67 expression level, a nuclear protein

linked to cell proliferation: the more it is expressed, the more the cells are proliferating. Thanks to these results it was understood that ZIP4 regulates PHLPP2 through miR-373 also *in vivo* and that miR-373 activity is related to tumor proliferation.

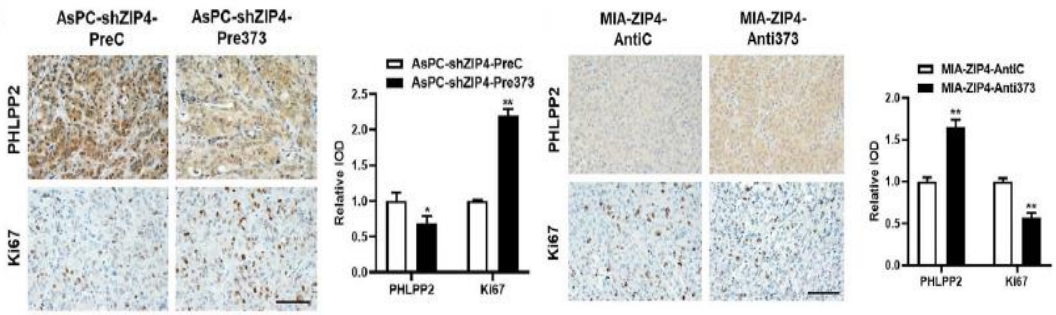

Figure 5: Immunohistochemistry of PHLPP2 protein expression level related to ZIP4/miR-373/Anti373 expression in vivo. Ki67 protein expression level as proliferation control.

Once decrypted the relationship between ZIP4 and PHLPP2 both *in vitro* and *in vivo* and knowing that PHLPP2 is involved in the phosphorylation state of AKT, the scientists tested the influence of ZIP4 on AKT phosphorilation state, exploiting koZIP4 cell model. As expected, koZIP4 cells presents higher expression of PHLPP2 and confirmed a lower phosphorylation of AKT (fig.9). This is explained since the PHLPP2 phosphatase activity with consequences on cell proliferation because acting on AKT.

Moreover, the role of circANAPC7-PHLPP2 axis on cell proliferation regulation was corroborated by further experiments. Transfecting ZIP4 overexpressing cells (MIA-ZIP4) with a circANAPC7 plasmidic expression vector, resulted in lower cell proliferation compared to the empty vector (EV) trasfected cells. Moreover, a

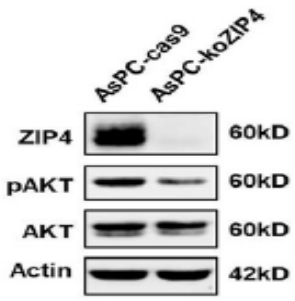

Figure 6: Western Blot assay indicates lower pAKT protein expression level in ZIP4KO cell line. Actin protein expression level as control.

decreased tumor mass is also observed in mice xenotransplanted with the same cell line (fig.10a). Furthermore, the same experiment was performed with AsPC cells that express miR-373 but ZIP4 is silenced (AsPC-shZIP4-Pre373), and transfected with circANAPC7 expression vector. In both cases researchers observed a reduction in in tumor mass growth (fig.10b) confirming the results obtained *in vitro*.

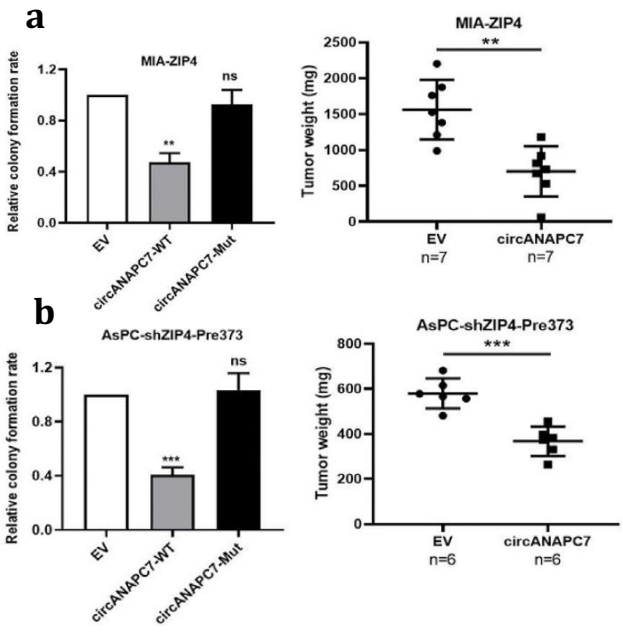

Figure 7: a) Colony formation assay showed CircANAPC7 anti-proliferative effects on ZIP4 over-expressed cells . b) Colony formation assay to see circANAPC7 effects on ZIP4 down-regulated and miR-373 up-regulated cells proliferation.

CyclinD1 is a circANAPC7 downstream target

Previous studies show cyclinD as a downstream target of ZIP4 in pacreatic cancer, since this molecule has a central role in cell proliferation, the authors decided to test a possible molecular relationship between cyclinD and circANAPC7. To clarify this point, a Western Blot was performed using an antibody

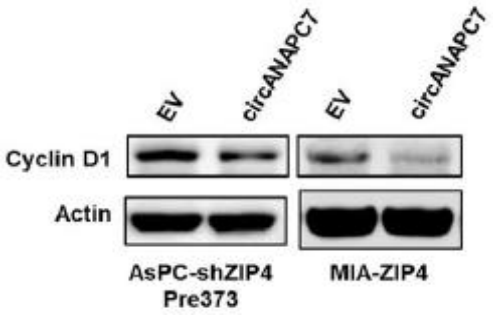

Figure 8: Western Blot assay indicates lower Cyclin D1 protein expression level when circANAPC7 is overexpressed in different pancreatic cancer cell lines. Actin protein expression level as housekeeping.

anti-cyclinD1 both on AsPC cells expressing only miR-373 (AsPC-shZIP4-Pre373) and on MIA cells overexpressing ZIP4 (MIA-ZIP4) both transfected with circANAPC7 . It has been obtained, in both on AsPC cells expressing miR-373, but not ZIP4 (AsPC-shZIP4-Pre373) and on MIA cells overexpressing ZIP4 (MIA-ZIP4), both transfected with circANAPC7 . It has been shown a depletion of cyclinD1 protein in both models, inferring that the decrease in the proliferation activity mediated by circANAPC7 could be due to the inhibition of cyclinD1 (fig.11).

Feed forward loop in CREB-miR-373-PHLPP2 signaling axis

Knowing already that ZIP4 activates miR-373 transcription via the phosphorylation state of CREB and knowing that PHLPP2 has phosphatase activity which acts against pAKT, another downstream target of ZIP4. Researchers wondered whether the activity of CREB and PHLPP2 were associated.

Mr. Min Li and his team exposed AsPC-1 cell line to 2 different experimental conditions in which, in the first, PHLPP2 was silenced using siPHLPP2, while, in the second, PHLPP2 was overexpressed through the transfection of circANAPC7. The obtained Western Blot results confirmed the relationship between the PHLPP2 phosphatase activity and the CREB phosphorylation status (fig.12).

This leads the researchers to think about a positive feedback process in which the activation of ZIP4 allows the expression of miR-373 by pCREB which in turn its dephosphorylation is less frequent due to the inhibitory action of miR-373 on PHLPP2. Thanks to these experiments, Min Li group defined the molecular loop and molecular relations linking ZIP4, CREB, mir-373 and PHLPP2 in a pancreatic cancer scenario.

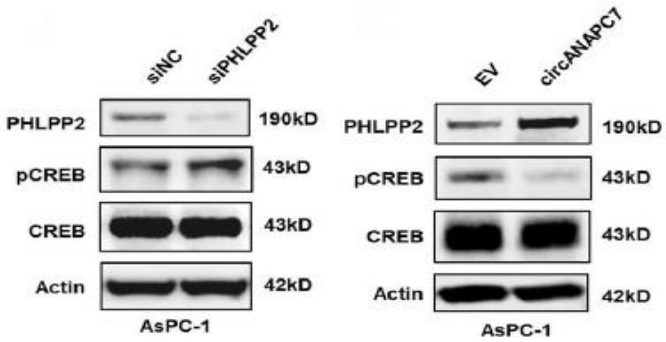

Figure 9: Western Blot of PHLPP2 and pCREB protein expression level related on shPHPP2/circANAPC7 transfected cells.. Actin protein expression level as housekeeping.

CircANAPC7 role in cachexia muscle wasting

In the applied experimental xenograft models, Mr. Min Li's team noticed how the weight of post-implanted mice with AsPC-shZIP4-Pre373-circANAPC7 cells was preserved when compared to the related controls (fig.10a). This led to think about an anti-cachectic role of circANAPC7 in this pancreatic tumor line. To confirm this evidence, weight (fig.13), fiber cross-sectional area (fig.13), and strength were measured in muscle collected from mice after AsPC-shZIP4-Pre373-circANAPC7 cells implantation. The results confirmed the scientists' hypothesis: both weight, strength and fiber size are preserved under circANAPC7 overexpression conditions in a pancreatic tumor context. This is the confirmation that circANAPC7 also plays an anti-cachectic as well as anti-cancer proliferation role.

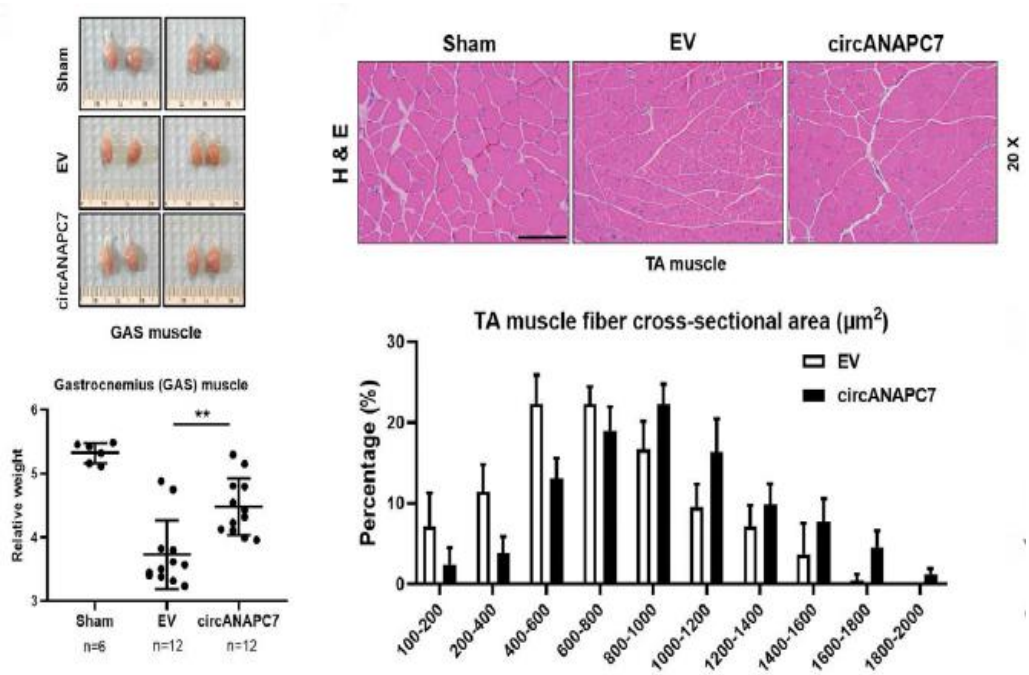

Figure 13: weight and fiber cross sectional area are preserved after circANAPC7 overexpressing cells implantation. Sham is a control surgery without cell implantation.

To understand circANAPC7 impact on ZIP4-mediated muscle wasting, the team treated C2C12 myotubes with a cell culture media exposed to AsPC-shZIP4-Pre373-circANAPC7 (conditioned media). Through WB, the expression levels of both cachectic markers, like UBR2, MuRF1 and Atrogin-1, and MyHC (myosin heavy chain) were tested. They observed an increase in MyHC levels with the presence of “circANAPC7 conditioned media” and a lower level of cachectic

markers among which we can observe Atrogin-1 in fig.14 (E3 subunit ubiquitination complex).

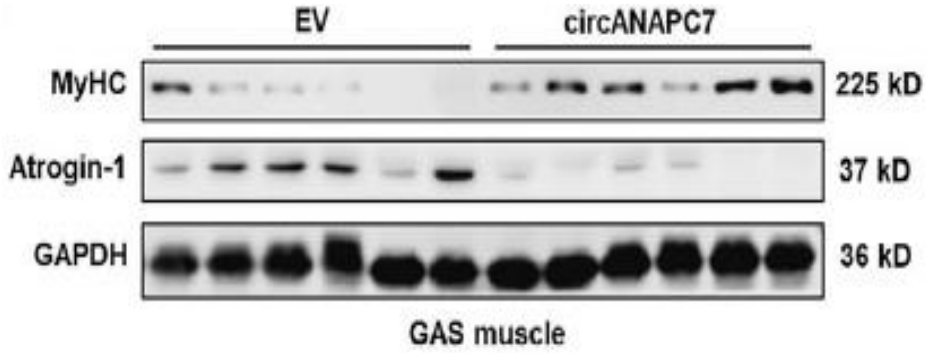

Figure 14: Western Blot of cachectic factor Atrogin-1 and muscle conservative factor MyHC protein expression level related to circANAPC7 over-expression. GAPDH expression level as housekeeping.

These results confirmed that the over-expression of circANAPC7 preserve muscle maintenance by inhibiting pancreatic cancer cachectic effect. Using a conditioned media experiment, they showed that their model of pancreatic tumor related cachexia is due to some soluble factor released by tumor cells.

Subsequently, it was decided to evaluate whether the multifunctional cytokine TGF-β, which can activate several pro-cachexia signaling pathways, was affected by the expression of circANAPC7. To clarify this point, TGF-β transcriptional and translational levels were evaluated in a context of circANAPC7 overexpression. They observed a significant decrease in TGF-β expression (fig.15a). For this reason, knowing that TGF-β is regulated by STAT5, which in turn is regulated by AKT, that is a circANAPC7-PHLPP2 downstream target; Mr. Min Li's group verified whether the level of STAT5 phosphorylation depends by circANAPC7 expression and

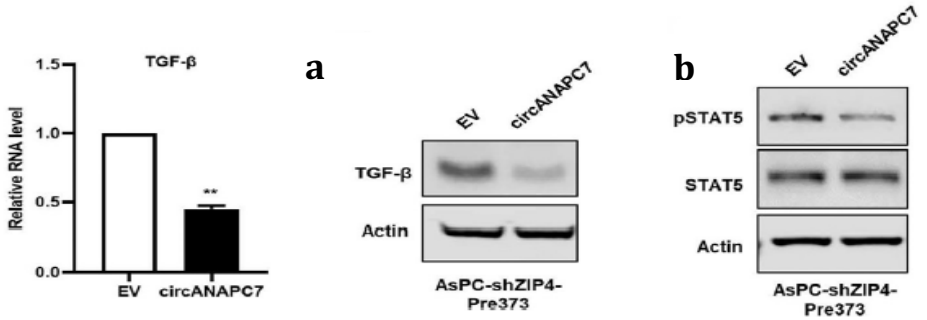

Figure 15: a) mRNA expression and protein level of TGF-β related to circANAPC7 up-regulation b) STAT5 phosphorylation level related to circANAPC7 over-expression in AsPC-shZIP4-Pre373 cells.

consequently by PHLPP2 activation. The results obtained by WB on AsPC-shZIP4-Pre373 cells transfected with circANAPC7 indicate a significant decrease in the phosphorylation state of STAT5 (Fig. 15b). This result indicated the possibility that circANAPC7 inhibits the transcription of TGF-β through the activation of PHLPP2 with consequent inhibition of AKT which can no longer activate STAT5, the transcriptional regulator of TGF-β. Thanks to this evidence, they concluded that the circANAPC7 anti-cachectic affect is mediated by the inhibition of the AKT-STAT5-TGF-β axis.

DISCUSSION

The authors of this paper recently discovered ZIP4 protein role in pancreatic cancer cell proliferation, metastasis, drug resistance, and cancer-associated cachexia. Consequently, Mr. Min Li's group conducted further investigations to better understand the signaling network involved in ZIP4-mediated pancreatic cancer progression with the purpose to discover potential molecular targets able to regulate it.

At the beginning of this study, the team worked *in silico* to discover some novel circular RNAs related to pancreatic cancer condition. They focused on this particular RNA family, since it seems to be a new potential target to regulate several signaling pathways.
During this research, a particular type of circular RNA called circANAPC7 was identified as possible ZIP4 signaling pathway regulator. Furthermore, they showed its inhibitory role on ZIP4-mediated cancer cell proliferation.

In this study, it has been used different typology of pancreatic cell lines and cultures. Moreover, proof of concept of several experiment has been proved *in vivo*, too.

The novelty showed in this paper is the circANAPC7 mediated degradation of miR-373, a phosphatase PHLPP2 transcriptional inhibitor. Furthermore, it was demonstrated that PHLPP2 acts on AKT signaling pathway mediating its inhibitory dephosphorylation. The latter results on lower levels of cyclinD1, a well-known AKT downstream cell proliferation stimulator. In this way, the authors showed for the first time, both *in vitro* and *in vivo*, the role of a novel discovered circular RNA able to reduce pancreatic cancer cell proliferation.

In this paper it is clearly shown a strong relation between circANAPC7 and CyclinD1. However, it is not demonstrated whether circANAPC7 act exclusively

through the AKT signaling to regulate CyclinD1. In my opinion, could be interesting to understand if our circular RNA could act also on CyclinD1 through AKT independent signaling pathways.

To clarify this issue, it could be interesting to build up some gene and protein expression experiments (e.g. real time PCR and western blot) on pancreatic cell lines presenting a KO or downregulation of AKT related signaling pathway, testing for CyclinD1 expression upon circANAPC7 overexpression.

This study has also clarified the ZIP4 downstream pathway involving a feedforward loop among the transcription factor CREB, miR373 and PHLPP2. In particular, the authors revealed that PHLPP2 mediates inhibitory dephosphorylation on CREB. To note, in pancreatic cancer condition, CREB is activated (phosphorylation) by ZIP4 allowing therefore miR-373 transcription promoting pancreatic cancer progression.

Investigating the pivotal role of circANAPC7 downstream ZIP4 mediated signaling pathways, the research group noticed that mice injected with circANAPC7 overexpressing pancreatic cancer cells, present a higher body mass. Therefore, inferring on a possible role of our circular RNA on pancreatic cancer mediated cachexia. In this paper is shown that the circANAPC7 cachexia protective effect is due a reduction on TGF-β secretion caused by lower amount of phosphorylated STAT5, highlighting that the latter is an AKT mediated post translational modification.

It would be interesting to investigate whether STAT5 dephosphorylation is directly due to the inhibitory action of PHLPP2 on AKT, or whether PHLPP2 could reduce pSTAT5 level directly or through signaling pathways not explored in this study.

In conclusion, this study demonstrated that circANAPC7 inhibits ZIP4-mediated pancreatic cancer cell proliferation and tumor cachexia. These results provide, for

the first-time, general insights into the role of circRNAs in pancreatic cancer progression and cachexia, suggesting a new potential therapeutic strategy to counteract pancreatic cancer progression and induced cachexia to improve patient prognosis.

BIBLIOGRAPHY

1. Karpińska M, Czauderna M. Pancreas-Its Functions, Disorders, and Physiological Impact on the Mammals' Organism. Front Physiol. 2022 Mar 30;13:807632. doi: 10.3389/fphys.2022.807632. PMID: 35431983; PMCID: PMC9005876.Arany, Z. (2008).

2. Jonathan D Mizrahi, Rishi Surana, Juan W Valle, Rachna T Shroff, Pancreatic cancer, The Lancet, Volume 395, Issue 10242, 2020, Pages 2008-2020, ISSN 0140-6736, https://doi.org/10.1016/S0140-6736(20)30974-0. https://www.sciencedirect.com/science/article/pii/S0140673620309740

3. Poulia KA, Sarantis P, Antoniadou D, Koustas E, Papadimitropoulou A, Papavassiliou AG, Karamouzis MV. Pancreatic Cancer and Cachexia-Metabolic Mechanisms and Novel Insights. Nutrients. 2020 May 26;12(6):1543. doi: 10.3390/nu12061543. PMID: 32466362; PMCID: PMC7352917.

4. Zhou, X., Wang, J.L., Lu, J., Song, Y., Kwak, K.S., Jiao, Q., Rosenfeld, R., Chen, Q., Boone, T., Simonet, W.S. and Lacey, D.L., 2010. Reversal of cancer cachexia and muscle wasting by ActRIIB antagonism leads to prolonged survival. *Cell*, *142*(4), pp.531-543.

5. Zhang Y, Bharadwaj U, Logsdon CD, Chen C, Yao Q, Li M. ZIP4 regulates pancreatic cancer cell growth by activating IL-6/STAT3 pathway through zinc finger transcription factor CREB. Clin Cancer Res. 2010 Mar 1;16(5):1423-30. doi: 10.1158/1078-0432.CCR-09-2405. Epub 2010 Feb 16. PMID: 20160059; PMCID: PMC2841320.

6. Balsano R, Kruize Z, Lunardi M, Comandatore A, Barone M, Cavazzoni A, Re Cecconi AD, Morelli L, Wilmink H, Tiseo M, Garajovà I, van Zuylen L, Giovannetti E, Piccirillo R. Transforming Growth Factor-Beta Signaling in Cancer-Induced Cachexia: From Molecular Pathways to the Clinics. Cells. 2022 Aug 28;11(17):2671. doi: 10.3390/cells11172671. PMID: 36078078; PMCID: PMC9454487.

7. Kordes M, Larsson L, Engstrand L, Löhr JM. Pancreatic cancer cachexia: three dimensions of a complex syndrome. Br J Cancer. 2021 May;124(10):1623-1636. doi: 10.1038/s41416-021-01301-4. Epub 2021 Mar 19. PMID: 33742145; PMCID: PMC8110983.

8. Yu T, Wang Y, Fan Y, Fang N, Wang T, Xu T, Shu Y. CircRNAs in cancer metabolism: a review. J Hematol Oncol. 2019 Sep 4;12(1):90. doi: 10.1186/s13045-019-0776-8. PMID: 31484561; PMCID: PMC6727394.

9. Su, M., Xiao, Y., Ma, J. *et al.* Circular RNAs in Cancer: emerging functions in hallmarks, stemness, resistance and roles as potential biomarkers. *Mol Cancer* **18**, 90 (2019). https://doi.org/10.1186/s12943-019-1002-6.

10. Kristensen, L.S., Jakobsen, T., Hager, H. *et al.* The emerging roles of circRNAs in cancer and oncology. *Nat Rev Clin Oncol* **19**, 188–206 (2022). https://doi.org/10.1038/s41571-021-00585-y.

Gastroenterology 2022;162:2004–2017

BASIC AND TRANSLATIONAL—PANCREAS

Circular RNA ANAPC7 Inhibits Tumor Growth and Muscle Wasting via PHLPP2–AKT–TGF-β Signaling Axis in Pancreatic Cancer

Xiuhui Shi,[1,2,*] **Jingxuan Yang**,[1,2,*] **Mingyang Liu**,[1,2,*] **Yuqing Zhang**,[1,2,*] **Zhijun Zhou**,[1,2,*] Wenyi Luo,[3] Kar-Ming Fung,[3] Chao Xu,[4] Michael S. Bronze,[1] Courtney W. Houchen,[1] and Min Li[1,2]

[1]Department of Medicine, University of Oklahoma Health Sciences Center, Oklahoma City, Oklahoma; [2]Department of Surgery, University of Oklahoma Health Sciences Center, Oklahoma City, Oklahoma; [3]Department of Pathology, University of Oklahoma Health Sciences Center, Oklahoma City, Oklahoma; and [4]Department of Biostatistics and Epidemiology, Hudson College of Public Health, University of Oklahoma Health Sciences Center, Oklahoma City, Oklahoma

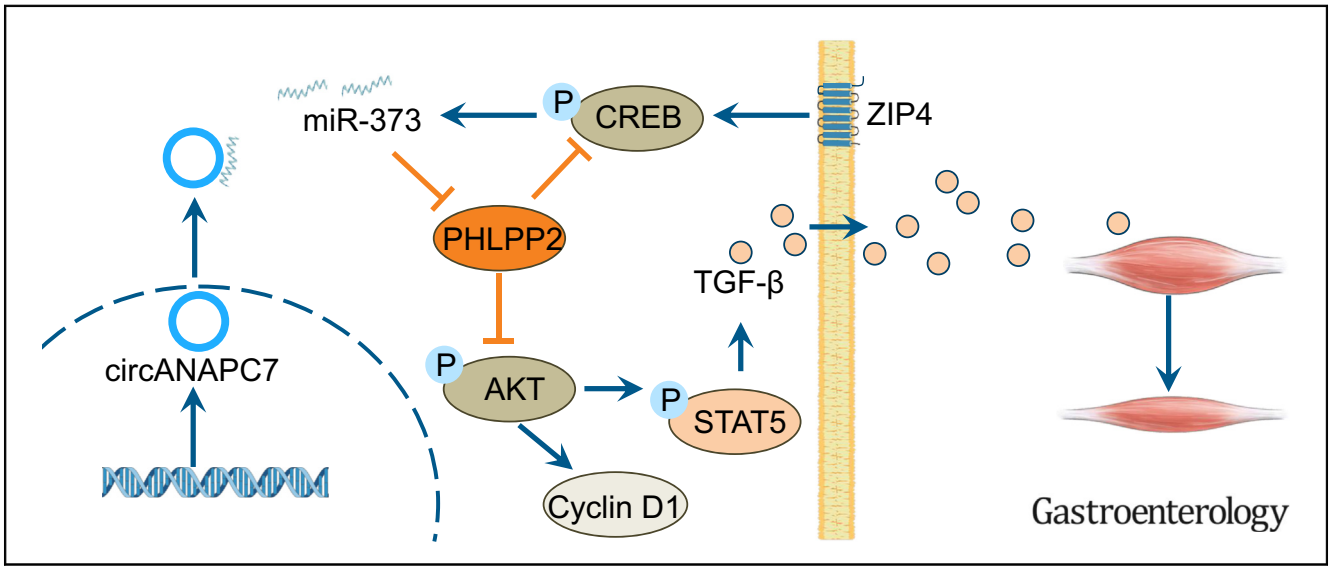

BACKGROUND & AIMS: Pancreatic cancer has the highest prevalence of cancer-associated cachexia among all cancers. ZIP4 promotes pancreatic cancer progression by regulating oncogenic miR-373, and perturbation of circular RNAs (circRNAs) is associated with cancer aggressiveness. This study aimed to identify circRNAs involved in ZIP4/miR-373–driven cancer growth and cachexia and decipher the underlying mechanism. **METHODS:** Differentially expressed circRNAs and potential targets of microRNA were identified through in silico analysis. The RNA interactions were determined by means of biotinylated microRNA pulldown, RNA immunoprecipitation, and luciferase reporter assays. The function of circRNA in ZIP4–miR-373 signaling axis were examined in human pancreatic cancer cells, 3-dimensional spheroids and organoids, mouse models, and clinical specimens. Mouse skeletal muscles were analyzed by means of histology. **RESULTS:** We identified circANAPC7 as a sponge for miR-373, which inhibited tumor growth and muscle wasting in vitro and in vivo. Mechanistic studies showed that PHLPP2 is a downstream target of ZIP4/miR-373. CircANAPC7 functions through PHLPP2-mediated dephosphorylation of AKT, thus suppressing cancer cell proliferation by down-regulating cyclin D1 and inhibiting muscle wasting via decreasing the secretion of transforming growth factor–β through STAT5. We further demonstrated that PHLPP2 induced dephosphorylation of CREB, a zinc-dependent transcription factor activated by ZIP4, thereby forming a CREB–miR-373–PHLPP2 feed-forward loop to regulate tumor progression and cancer cachexia. **CONCLUSION:** This study identified circANAPC7 as a novel tumor suppressor, which functions through the CREB–miR-373–PHLPP2 axis, leading to AKT dephosphorylation, and cyclin D1 and transforming growth factor–β down-regulation to suppress tumor growth and muscle wasting in pancreatic cancer.

Keywords: CircRNA; MicroRNA; Proliferation; Cachexia.

Pancreatic cancer is predicted to become the second leading cause of cancer-associated death in the United States by 2030, with a 5-year survival rate of no more than 10%.[1] Surgery plus chemotherapy provides the best chance of cure for patients with pancreatic cancer. Unfortunately, >80% of patients are diagnosed at advanced stages and are not eligible for surgery.[2] In addition, approximately 70% of patients with pancreatic cancer develop cancer cachexia, a systematic metabolic dysfunction characterized by body weight loss with ongoing muscle wasting (with or without adipose loss), which cannot be reversed by conventional nutritional support.[3,4] Muscle wasting is the major hallmark of cancer cachexia caused by substantially increased muscle protein breakdown.[5] Cancer cachexia reduces quality of life, decreases tolerance to chemotherapy, and ultimately leads to tumor progression in patients with pancreatic cancer.[3] However, there is no effective treatment for cancer-associated cachexia and the underlying mechanism remains mostly unclear. Therefore, there is an urgent need to further explore the biology and molecular mechanism of pancreatic cancer progression and develop efficient therapeutic targets.

Zinc is an essential metal ion and nutrient that plays important physiological and pathologic roles.[6] Abnormal zinc homeostasis is associated with increased cell death and resistance to chemotherapy in pancreatic cancer.[7] Therefore, illustrating the mechanism of aberrant expression of zinc transporter and its regulation in pancreatic cancer may lead to more effective therapeutics.[8] We recently found that ZIP4 plays critical roles in cell proliferation, metastasis, drug resistance, and cancer-associated cachexia in pancreatic cancer.[9–14] Therefore, it is crucial to further explore the signaling network on ZIP4-induced cancer progression and cachexia to develop novel therapeutic strategies for pancreatic cancer.

Circular RNA (circRNA) is a closed-loop RNA with a junction between the 3′ and 5′ ends from reverse splicing of precursor messenger RNA (mRNA).[15] MicroRNA (miRNA) is a class of small noncoding RNA involved in multiple biological processes by inhibiting the translation of mRNA.[16] The miRNA sponge is an RNA transcript with complementary binding sites to this specific miRNA, thus inhibiting the function of the miRNA.[17] CircRNAs sponge miRNAs more effectively, as they are more stable and have more binding sites than linear RNAs.[18] CircRNAs are involved in multiple functions of pancreatic cancer, including tumor growth, differentiation, apoptosis, invasion, metastasis, lymph angiogenesis, and chemotherapy resistance.[19–22] However, the mechanism of circRNA in pancreatic cancer remains largely elusive, especially in the context of ZIP4-mediated tumor progression. Previously, we showed that the expression of an oncogenic miRNA, miR-373, is regulated by ZIP4 and is essential for ZIP4-induced pancreatic cancer progression. However, whether circRNAs could act as miR-373 sponges, and their impact on ZIP4 signaling, is unknown.

WHAT YOU NEED TO KNOW

BACKGROUND AND CONTEXT

ZIP4 promotes pancreatic cancer progression by regulating miR-373. Perturbation of circular RNAs (circRNAs) is associated with cancer aggressiveness. We aimed to identify circRNAs involved in ZIP4/miR-373–driven cancer cachexia and decipher the underlying mechanism.

NEW FINDINGS

CircANAPC7 is a tumor suppressor that functions through PHLPP2-mediated dephosphorylation of AKT, resulting in down-regulation of cyclin D1 and transforming growth factor–β. PHLPP2 also induced dephosphorylation of CREB, a zinc-dependent transcription factor activated by ZIP4, thus forming a CREB–miR-373–PHLPP2 feed-forward loop to regulate cancer progression and cachexia.

LIMITATIONS

The role of other miR-373–related circRNAs were not included in this study.

IMPACT

This study identifies CircANAPC7 as a novel tumor suppressor and provides a potential therapeutic strategy to suppress tumor growth and muscle wasting in pancreatic cancer.

In the present study, we found that circRNA ANAPC7 suppressed pancreatic cancer growth and ameliorated cachexia by sponging miR-373. We identified PHLPP2, a protein phosphatase involved in the regulation of AKT signaling, as a novel miR-373 target gene in pancreatic cancer. Furthermore, we found that PHLPP2 decreased CREB phosphorylation, a zinc-dependent transcription factor regulated by ZIP4, which promotes miR-373 expression by transcriptional regulation. We identified an uncharacterized CREB–miR-373–PHLPP2 feed-forward loop of the ZIP4-mediated signaling axis in pancreatic cancer. Moreover, we found circANAPC7 ameliorated cachexia by reversing ZIP4-induced muscle wasting through down-regulating transforming growth factor (TGF)-β expression and secretion via STAT5. Our findings suggest novel insights on circANAPC7 in ZIP4-mediated pancreatic cancer progression and cachexia, thus providing a potential therapeutic strategy for cancer treatment and clinical management of cancer cachexia.

*** Authors share co-first authorship.**

Abbreviations used in this paper: **circRNA, circular RNA; 2D, 2-dimensional; 3D, 3-dimensional; DEC, differentially expressed circular RNA; HPDE, human pancreatic duct epithelial; IHC, immunohistochemistry; mRNA, messenger RNA; MyHC, myosin heavy chain; RT-qPCR, reverse transcription quantitative real-time polymerase chain reaction; TGF, transforming growth factor.**

Most current article

0016-5085
https://doi.org/10.1053/j.gastro.2022.02.017

Materials and Methods

Cell Lines and Clinical Specimens

Human pancreatic cancer cell lines AsPC-1, MIA PaCa-2, BxPC-3, Panc-1, and CFPAC-1 were purchased from American Type Culture Collection. The human pancreatic duct epithelial (HPDE) cell line was a gift from Dr Ming-Sound Tsao (Ontario Cancer Institute).[23] These cells were cultured as described previously.[9] MIA-V/ZIP4, MIA-ZIP4-anti-C/anti-373, AsPC-shV/shZIP4, AsPC-shZIP4-PreC/Pre373 stable cell lines were constructed in our laboratory previously.[10] MIA-V/ZIP4, MIA-ZIP4-anti-C/anti-373 cells were cultured in complete media supplemented with 0.5 μg/mL puromycin (#A1113803; Gibco). AsPC-shV/shZIP4, AsPC-shZIP4-PreC/Pre373 cells were cultured in complete media supplemented with 1 μg/mL puromycin. Murine C2C12 myoblasts (American Type Culture Collection) were cultured in Dulbecco's modified Eagle medium supplemented with 10% fetal bovine serum. All cells were cultured at 37°C under 5% CO_2. Banked de-identified human pancreatic cancer tissue specimens were obtained from the University of Oklahoma Health Sciences Center according to an approved Institutional Review Boards human protocol. Written consent was obtained from all subjects.

3-Dimensional Spheroid and Organoid Culture

The 3-dimensional (3D) spheroid and organoid cultures were performed as described previously.[13,14] Briefly, pancreatic cancer cells were resuspended in medium containing 0.24% methylcellulose (#M0512; Sigma-Aldrich). Cells were seeded on the inner lid of a 10-cm Petri dish with 20 μL per drop. The lid was put on the Petri dish containing 10 mL phosphate buffer solution. The suspended droplets were incubated for 5–7 days in 5% CO_2 at 37°C to form 3D cell spheroids. Matrigel-based 3D embedded and suspended organoids were generated based on a similar method, except that the cell suspension was mixed with Matrigel (#354234; Corning). The spheroids were embedded with HistoGel and paraffin, then sectioned for H&E staining.

Biotinylated MicroRNA Pulldown Assay

The miRNA pulldown assay was performed as described by Lal et al.[24] Briefly, the 3′ end biotinylated miRCURY LNA Premium miRNA Mimic or control RNA (#39178/3BIO; Qiagen) were transfected into cells at a final concentration of 30 nM for 24 hours. The cells were washed with phosphate-buffered saline and incubated in lysis buffer. The biotin-coupled RNA complex was pulled down by incubating the cell lysates with Dynabeads MyOne Streptavidin T1 (#65601; Invitrogen). The beads were blocked with RNase-free bovine serum albumin (#AM2616; Invitrogen) and yeast transfer RNA (#15401029, Invitrogen) on a rotator at 4°C for 2 hours to prevent nonspecific binding of RNA and protein complexes. The blocked beads were incubated with cell lysates at 4°C overnight, washed 3 times with ice-cold lysis buffer. The RNA complexes on the beads were eluted and extracted by TRIzol reagent (#15596026; Invitrogen). The abundance of circANAPC7 and miR-373 of RNA complexes was evaluated by reverse transcription quantitative real-time polymerase chain reaction (RT-qPCR) analysis.

RNA Immunoprecipitation

miRNA mimics were transfected into cells for 24 hours after transfection, and AGO2 antibody (#SAB4200085; MilliporeSigma) or negative control IgG antibody (#10500C; Invitrogen) was used to perform AGO2 immunoprecipitation. Cells were lysed in cOmplete Lysis-M (#04719956001; Roche) supplemented with protease inhibitor (#04693116001; Roche) and RNase inhibitor (#AM2694; Invitrogen) for 10 minutes. The antibodies were incubated with Dynabeads magnetic beads of a Dynabeads Protein G Immunoprecipitation Kit (#10007D; Invitrogen) at room temperature for 30 minutes. The lysate was mixed with antibody-beads complexes and incubated under rotation overnight at 4°C. After treating with proteinase K (#03115836001; Roche), RNA complexes were extracted using TRIzol reagent. The abundance of RNAs was evaluated by RT-qPCR analysis.

Luciferase Reporter Assay

Luciferase reporter assay was performed using the Dual-Luciferase Reporter Assay System (#E1960; Promega) following the manufacturer's protocol. Briefly, cells were seeded in a 24-well plate and co-transfected with the plasmid of 500 ng and miRNA mimics of 10 pmol per well using Lipofectamine 3000 Reagent (#L3000015; Invitrogen). At 48 hours after transfection, the cells were lysed and firefly luciferase activity and Renilla luciferase activity were measured using a Microplate Reader (Synergy H1; BioTek).

RNA Location Assay

The nuclear and cytoplasmic RNAs were extracted using the Nuclear and Cytoplasmic Extraction Kit (PARIS, AM1921; Invitrogen). One picogram of DNA spike-in molecules was added to each sample for RT-qPCR normalization. DNA spike-in was produced from the multiple cloning sites in pcDNA3.1(+) CircRNA Mini Vector (#60648; Addgene).

Transcription Block Assay

Transcription was blocked by adding 2 μg/mL actinomycin D (A1410; Sigma-Aldrich) or dimethyl sulfoxide control to the cell culture medium and cultured for 0, 4, 8, 12, or 24 hours. Then the cells were harvested and total RNA was extracted. The stability of circANAPC7 and ANAPC7 mRNA was analyzed by means of RT-qPCR.

Ribonuclease R Treatment

The total RNA was incubated with or without 2 U/μg ribonuclease R (#RNR07250; Epicentre Technologies) for 15 minutes at 37°C and purified using the RNeasy MinElute Cleanup Kit (#74204; Qiagen), then analyzed by RT-qPCR.

Orthotopic Xenograft Mouse Model

MIA-ZIP4-EV/circANAPC7, AsPC-shZIP4-Pre373-EV/circANAPC7 stable cell lines were used to establish the pancreatic cancer orthotopic xenograft mouse model as described previously.[10] Briefly, 3×10^6 cells in 50 μL Dulbecco's modified Eagle medium or RPMI medium were injected into the tail of the pancreas of 5-week athymic nude mice. The mice study was performed under an animal protocol approved by the Animal

Welfare Committee at University of Oklahoma Health Sciences Center. Four weeks post injection, mice were euthanized and tissues were collected.

Statistical Analysis

Statistical analysis was performed with Prism 8 (GraphPad Software). Comparisons of 2 groups were conducted using a 2-tailed Student *t* test. One-way analysis of variance was used for multiple conditions compared for 1 variable. Two-way analysis of variance was performed for multiple sets of multivariate comparisons. A P value $< .05$ was considered statistically significant.

Results

CircANAPC7 Acts as a miR-373 Sponge in Pancreatic Cancer Cells

To identify the potential circRNA that acts as a miR-373 sponge, we analyzed differentially expressed circRNAs (DECs) from the circRNA microarray dataset of pancreatic cancer and screened circRNAs with miR-373 binding sites from circBank online database.[25,26] We identified 223 up-regulated DECs and 214 down-regulated DECs (Supplementary Table 1) in pancreatic cancer, and the top 100 DECs are shown in Figure 1*A*. Among the 214 down-regulated DECs, we focused on 5 circRNAs containing miR-373 binding sites for further investigation (Supplementary Figure 1*A*). To validate which circRNA interacts with miR-373, we performed miRNA pulldown assay and found only hsa_circ_0005785 (also known as circANAPC7) was enriched in the miR-373–captured fraction compared with the negative control, indicating miR-373 could interact with circANAPC7 in pancreatic cancer cells (Figure 1*B*, Supplementary Figure 1*B*). Next, we confirmed the circular structure of circANAPC7, derived from exon 3 to exon 9 of a protein-coding gene ANAPC7, in pancreatic cancer cell lines by Sanger sequencing and PCR analysis (Figure 1*C* and Supplementary Figure 1*C*). We found that circANAPC7 was down-regulated in pancreatic cancer cells compared with HPDE cells (Supplementary Figure 1*D*). Consistent with the circRNA microarray results, circANAPC7 level was significantly lower in human pancreatic cancer tissues than tumor-adjacent tissues (Supplementary Figure 1*E*). The analysis of nuclear and cytoplasmic circANAPC7 revealed that circANAPC7 is preferentially localized to the cytoplasm (Figure 1*D*). To analyze the stability of circANAPC7 and ANAPC7 mRNAs, we treated pancreatic cancer cells with actinomycin D, an inhibitor of transcription, and found that circANAPC7 transcript is more stable than linear ANAPC7 mRNA transcript (Supplementary Figure 1*F*). Furthermore, we found circANAPC7 was resistant to ribonuclease R exonuclease digestion, which further supported the circular structure of this RNA transcript (Supplementary Figure 1*G*). We next determined whether circANAPC7 serves as a binding platform for miR-373 and AGO2, the essential component in the process of miRNA repression of specific target RNA. We performed RNA immunoprecipitation of AGO2 in pancreatic cancer cells transfected with miR-373 mimics and found that endogenous circANAPC7 was enriched in the AGO2 group (Figure 1*E*). We further constructed luciferase reporter vectors by inserting circANAPC7 wild-type or mutant fragment right behind the reporter gene (Figure 1*F*) and found a significantly decreased luciferase activity in the circANAPC7 wild-type group compared with the circANAPC7 mutant group in miR-373 overexpressed cells (Figure 1*G*). These results suggest that circANAPC7 binds to miR-373 and may serve as a miR-373 sponge to suppress its function in pancreatic cancer.

CircANAPC7 Inhibits Pancreatic Cancer Cell Proliferation in 2-Dimensional and 3-Dimensional Models

To further investigate the function of circANAPC7, we overexpressed circANAPC7 in AsPC-1 and MIA PaCa-2 cells (Supplementary Figure 2*A*). Overexpression of circANAPC7 significantly suppressed pancreatic cancer cell proliferation and colony formation (Figure 2*A* and *B*). The 5-ethynyl-2′-deoxyuridine incorporation assay revealed that circANAPC7 overexpression impaired DNA synthesis in human pancreatic cancer cells (Figure 2*C*). We also observed a similar inhibitory effect of circANAPC7 on cell growth in 3D spheroid and organoid models. CircANAPC7 showed no significant impact on the aggregation of spheroids, however, circANAPC7 overexpression inhibited spheroid growth compared with the control group (Supplementary Figure 2*B–D* and Figure 2*D*). Consistent with 2D culture and 3D spheroids, circANAPC7 overexpression suppressed the growth of organoids in both Matrigel-suspended and Matrigel-embedded culture conditions (Figure 2*E*, Supplementary Figure 2*E*). These results demonstrated that circANAPC7 inhibits pancreatic cancer cell growth as a tumor suppressor.

PHLPP2 Is a Downstream Target of miR-373

To identify the downstream targets responsible for mediating the oncogenic function of miR-373, we analyzed the human tumor suppressor genes with miR-373 binding sites and found 18 genes occurred simultaneously within the 3 categories (Figure 3*A* and Supplementary Figure 3*A*). Among the 18 potential downstream targets of miR-373, we selected 3 candidates (SASH1, PHLPP2, and PAFAH1B1) for further validation because they are negatively correlated with ZIP4 in human pancreatic cancer tissues (Supplementary Figure 3*B–D*). Then we evaluated whether circANAPC7 regulates miR-373 target gene expression through sponging miR-373. The RT-qPCR analysis demonstrated that overexpression of circANAPC7 up-regulated the mRNA level of PHLPP2 but not SASH1 or PAFAH1B1 (Figure 3*B* and *C*). CircANAPC7 overexpression also increased the protein level of PHLPP2 in pancreatic cancer cells (Figure 3*D*, Supplementary Figure 3*E*). miR-373 blocking up-regulated PHLPP2, while miR-373 overexpression down-regulated PHLPP2 (Figure 3*E* and Supplementary Figure 3*F–H*). These results indicated that circANAPC7 serves as a miR-373 sponge to regulate PHLPP2

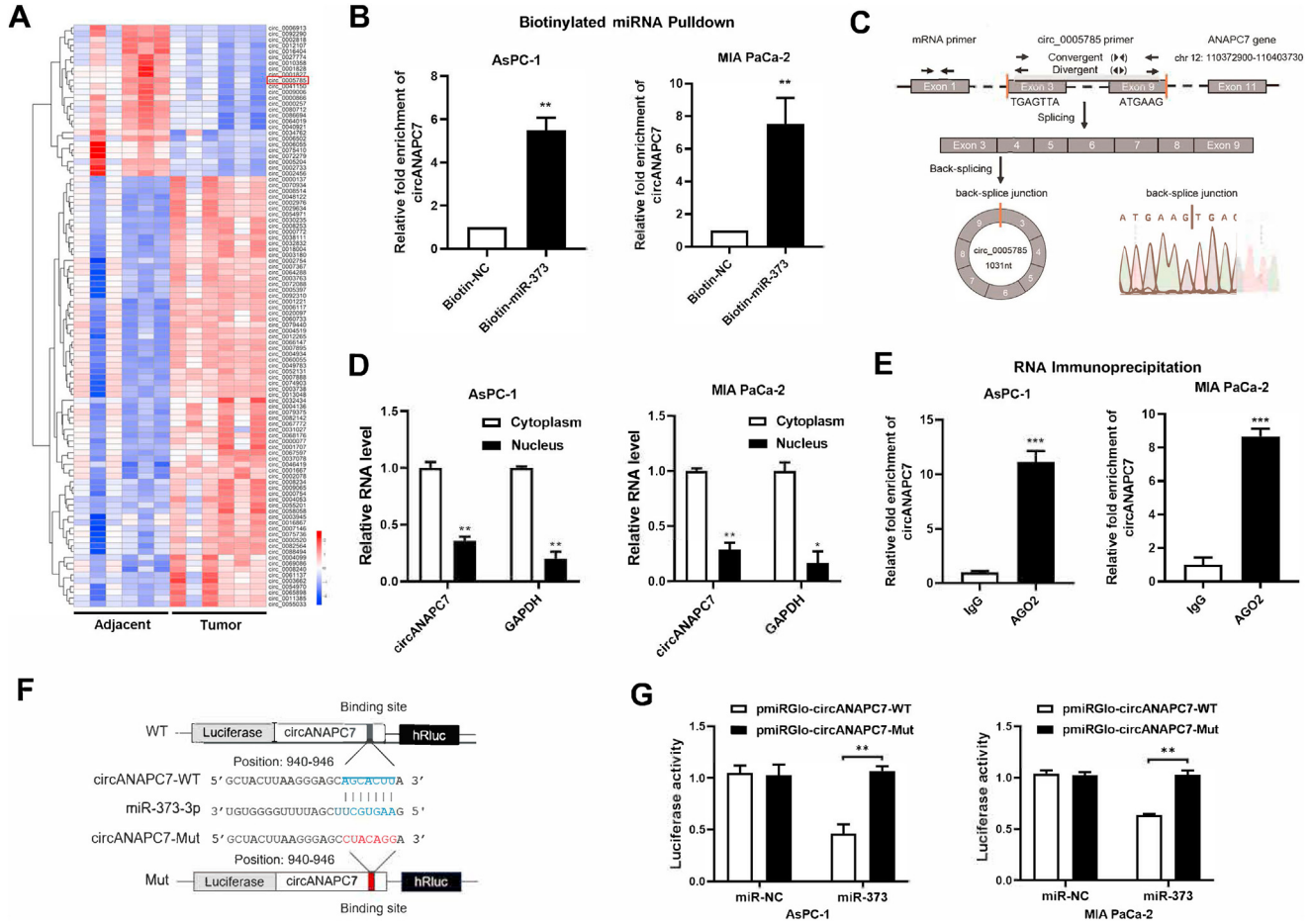

Figure 1. CircANAPC7 interacts with miR-373 in pancreatic cancer cells. (*A*) *Heatmap* of the top 100 differentially expressed circRNAs between 6 pairs of pancreatic cancer and adjacent tissues (GSE69362). (*B*) CircANAPC7 levels detected by RT-qPCR analysis of miRNA pulldown products. (*C*) CircANAPC7 structure and the validation strategy. (*D*) CircANAPC7 and GAPDH mRNA level in pancreatic cancer cells. (*E*) RNA immunoprecipitation assay was performed with cell lysate of AsPC-1 and MIA PaCa-2 cells transfected with miR-373 mimics using either anti-AGO2 or IgG as the immunoprecipitating antibody. (*F*) *Schematic diagram* of luciferase reporter vectors with circANAPC7 wild-type (WT) (*blue*) or mutated (Mut) (*red*) putative miR-373 binding sites. (*G*) Luciferase activity of circANAPC7 reporter vectors (WT and Mut) co-transfected with negative control (NC) or miR-373 mimics in AsPC-1 and MIA PaCa-2 cells. Firefly luciferase activity was normalized to Renilla luciferase activity. *Error bars* represent SDs. **P* < .05; ***P* < .01; ****P* < .001.

expression in pancreatic cancer cells. To examine whether miR-373 binds to the 3′UTR of PHLPP2, we performed a biotin-labeled miR-373 pulldown assay and found an 8-fold enrichment of the 3′UTR of PHLPP2 (Figure 3*F*). We also used the luciferase reporter system to detect whether miR-373 regulated the expression of PHLPP2 by binding to its 3′UTR. We cloned the PHLPP2-3′UTR with wild-type or mutant miR-373–binding site right behind the luciferase reporter vector for the luciferase reporter assay (Figure 3*G*) and observed that miR-373 expression could reduce luciferase activity of the wild-type PHLPP2-3′UTR reporter vector, but not the mutant reporter vector (Figure 3*H*). Collectively, these data suggested that PHLPP2 is a downstream target of miR-373, and circANAPC7 increased the PHLPP2 level by sponging miR-373.

We further examined whether circANAPC7 suppresses pancreatic cancer cell proliferation by up-regulating PHLPP2. Cell viability assays showed that miR-373–induced cell proliferation was partially reversed by wild-type, but not mutant, circANAPC7 (Figure 3*I*). In addition, 5-ethynyl-2′-deoxyuridine incorporation assays also revealed that the wild-type, but not mutant, circANAPC7 could reverse miR-373–mediated increase of DNA synthesis (Figure 3*J*). PHLPP2 was recently identified as an important regulator of AKT, functioning as an AKT-Ser473 phosphatase and resulting in AKT inactivation.[27] We also observed phosphorylated AKT level was increased after PHLPP2 silencing, but decreased by PHLPP2 overexpression in pancreatic cancer cells (Supplementary Figure 4*A*–*F*). The overexpression of miR-373 significantly decreased the PHLPP2 level and increased phosphorylated AKT, and these effects were reversed by wild-type circANAPC7 overexpression under both 2D culture and 3D spheroid culture conditions (Figure 3*K*). Furthermore, PHLPP2 silencing attenuated the inhibition of cancer cell growth by circANAPC7 (Figure 3*L* and *M*). CircANAPC7–mediated inhibition

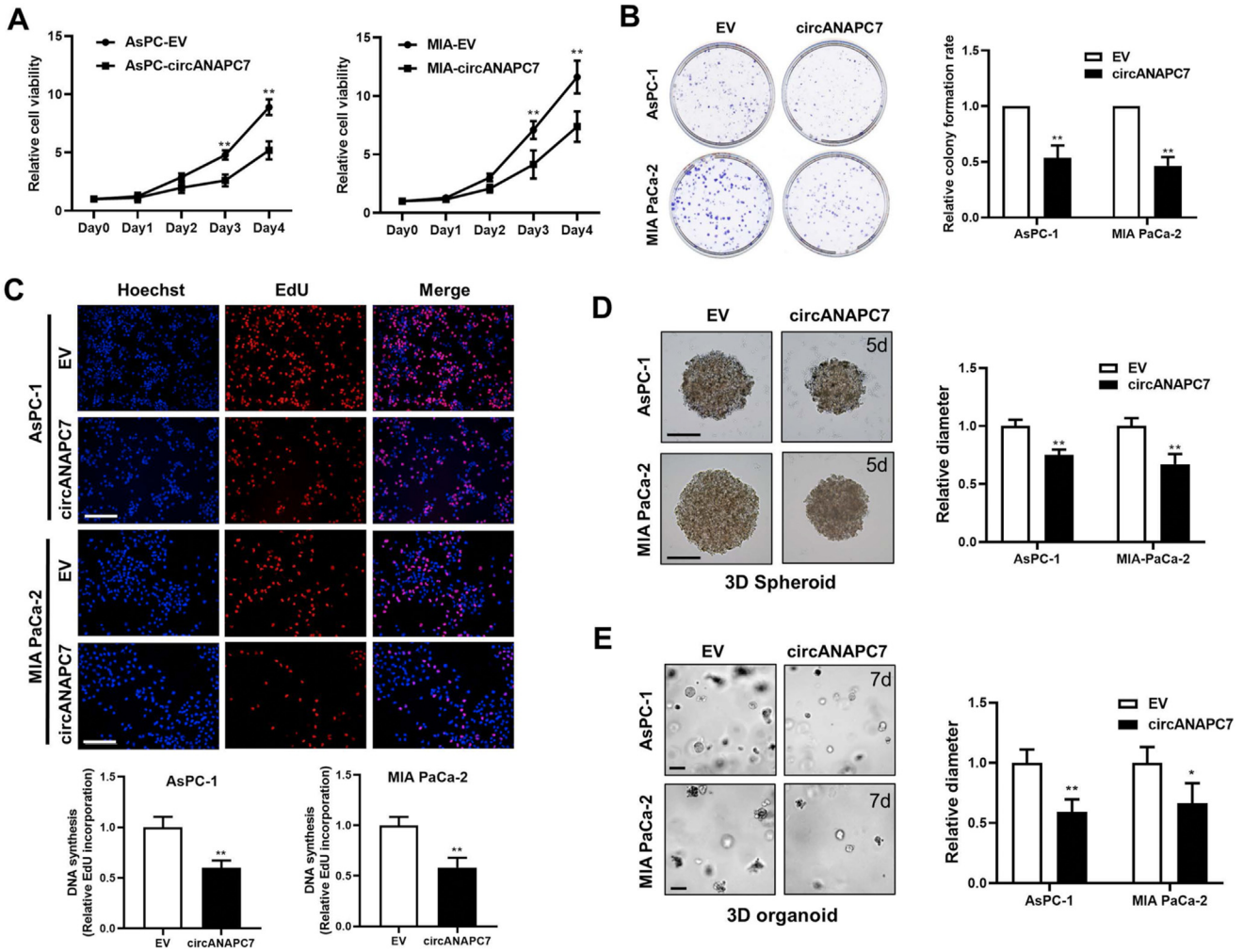

Figure 2. CircANAPC7 inhibits pancreatic cancer cell growth in 2D and 3D cultures. (*A*) Cell viability of AsPC-EV/circANAPC7, MIA-EV/circANAPC7 cells were assessed using the MTT reagent at the indicated days. (*B*) Colony-formation assay (*left panel*). The analysis of relative colony-formation rate (*right panel*). (*C*) DNA synthesis assessed using a 5-ethynyl-2′-deoxyuridine (EdU) assay in indicated cells (*top panel*). *Scale bar:* 100 μm. Quantitative data of EdU assay (*bottom panel*). (*D*) Representative *images* of methylcellulose-based 3D cancer cell spheroids established from AsPC-EV/circANAPC7, MIA-EV/circANAPC7 cells cultured for 5 days. *Scale bar:* 200 μm. (*E*) Representative *images* of Matrigel-suspended 3D organoids established from AsPC-EV/circANAPC7, MIA-EV/circANAPC7 cells cultured for 7 days. *Scale bar:* 50 μm. $^{*}P < .05$; $^{**}P < .01$.

of AKT phosphorylation was also attenuated by PHLPP2 silencing (Figure 3*N*). These results demonstrated that circANAPC7 suppressed pancreatic cancer cell proliferation through miR-373/PHLPP2.

ZIP4 Inhibits PHLPP2 Expression by Activating miR-373

The expression of miR-373 is regulated by ZIP4 through a zinc-dependent transcription factor CREB, as we demonstrated previously.[10] The survival analysis of miR-373 target gene PHLPP2 in The Cancer Genome Atlas database showed that PHLPP2 is a prognostic marker in pancreatic cancer. Patients with a lower level of PHLPP2 had a worse prognosis in pancreatic cancer (5-year survival, low vs high: 15% vs 34%, $P = .0002$, Figure 4*A*). Thus, we further investigated whether ZIP4 regulates expression of PHLPP2. We observed that ZIP4 knockout increased both mRNA and protein levels of PHLPP2, while ZIP4 overexpression decreased PHLPP2 levels (Supplementary Figure 5*A*–*C* and Figure 4*B*). Furthermore, the protein level of PHLPP2 was reduced in pancreatic cancer stable cells with ZIP4 knockdown and miR-373 overexpression, while PHLPP2 level increased in miR-373 blocked pancreatic cancer cells after ZIP4 overexpression (Figure 4*C* and *D* and Supplementary Figure 5*D* and *E*). Accordingly, the PHLPP2 level was decreased by miR-373 mimics and increased by anti–miR-373 oligonucleotides transfection with or without ZIP4 present in MIA-ZIP4 and AsPC-koZIP4 cells (Figure 4*E* and *F* and Supplementary Figure 5*F* and *G*). Next, we confirmed the regulatory role of the ZIP4–miR-373–PHLLP2 signaling axis in pancreatic tumor growth using an orthotopic xenograft mouse model. Immunohistochemistry (IHC) staining showed that tumor tissues of the AsPC-shZIP4-Pre373 group had higher levels of Ki67 but lower levels of PHLPP2 compared with the AsPC-shZIP4-PreC group (Figure 4*G*).

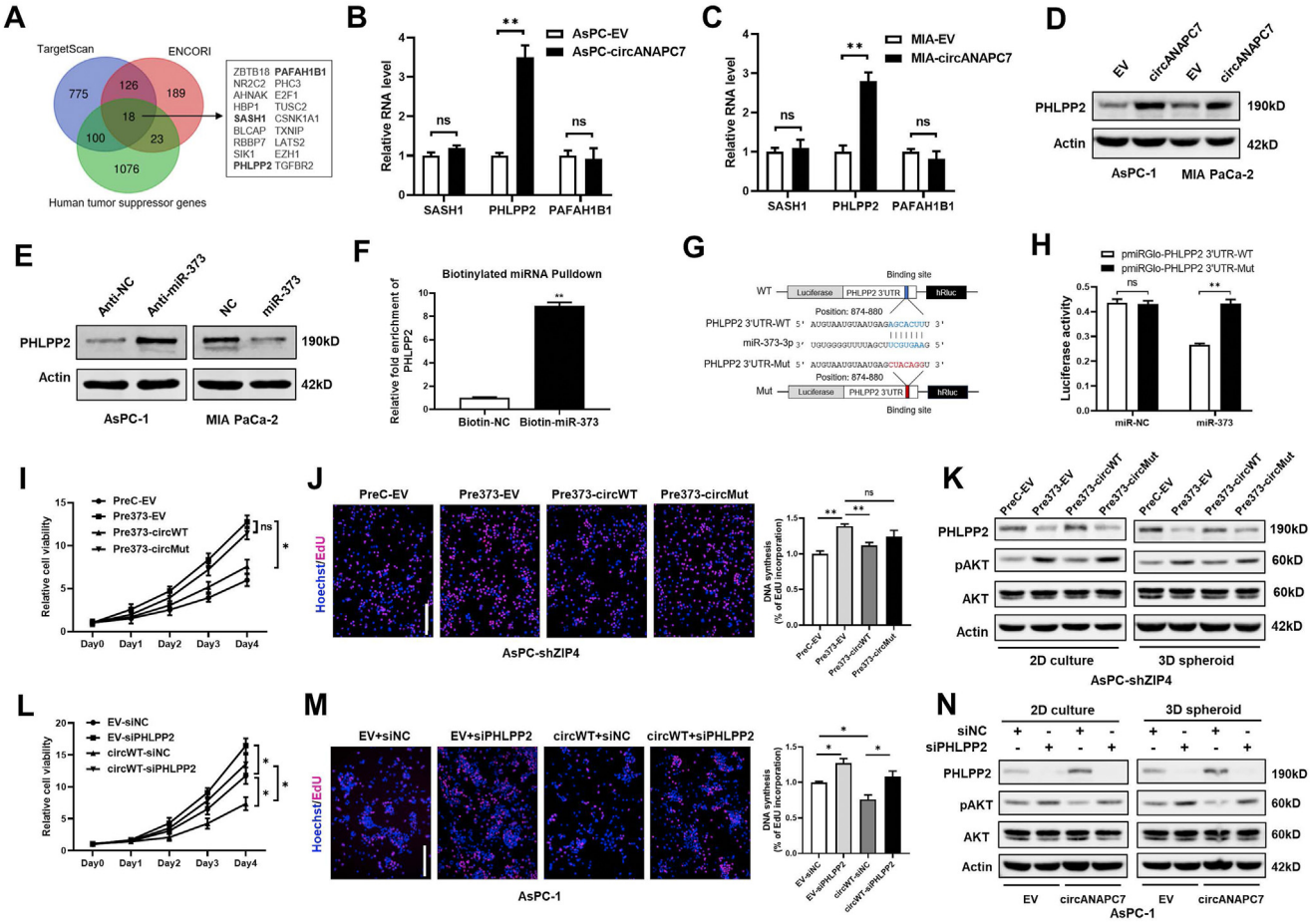

Figure 3. CircANAPC7 inhibits cell proliferation by serving as a miR-373 sponge to increase PHLPP2 level in pancreatic cancer. (*A*) *Schematic diagram* showing the identification of tumor suppressor genes that contain predicted binding sites of miR-373 in indicated databases. (*B*) mRNA levels of SASH1, PHLPP2, and PAFAH1B1 in AsPC-EV/circANAPC7 cells. (*C*) mRNA levels of SASH1, PHLPP2, and PAFAH1B1 in MIA-EV/circANAPC7 cells. (*D*) PHLPP2 protein levels in AsPC-EV/circANAPC7, MIA-EV/circANAPC7 cells. (*E*) PHLPP2 protein levels in AsPC-1 cells transfected with anti-NC/miR-373 oligonucleotides (*left panel*). PHLPP2 protein levels in MIA PaCa-2 cells transfected with miR-NC/miR-373 mimics (*right panel*). (*F*) RT-qPCR analysis of RNA pulldown products detecting PHLPP2 mRNA level in the streptavidin captured fractions from the MIA PaCa-2 cell lysates after transfection with biotinylated miR-373 or NC probes. (*G*) *Schematic diagram* of PHLPP2-3′UTR reporter vectors. (*H*) Luciferase activity of PHLPP2-3′UTR reporters (WT and Mut) co-transfected with NC or miR-373 mimics in MIA PaCa-2 cells. (*I*) Cell viability was assessed by MTT. (*J*) DNA synthesis was assessed by 5-ethynyl-2′-deoxyuridine (EdU) assay. (*K*) Protein levels of PHLPP2, pAKT, and total AKT. (*L*) Cell viability was assessed by MTT. (*M*) DNA synthesis was assessed by EdU assay. (*N*) Protein level of PHLPP2, pAKT, and total AKT in AsPC-EV/circANAPC7 stable cells transfected with small interfering RNAs of PHLPP2 or control under 2D culture and 3D spheroid culture. circWT, circANAPC7-WT; circMut, circANAPC7-Mut; NC, negative control; ns, not significant; *$P < .05$; **$P < .01$.

Compared with the MIA-ZIP4-anti-C group, tumor tissues of the MIA-ZIP4-anti-373 group had a lower level of Ki67 and a higher level of PHLPP2 (Figure 4*H*). To further analyze the downstream of the ZIP4-miR-373-PHLLP2 signaling axis, we performed Kyoto Encyclopedia of Genes and Genomes pathway analysis on differentially expressed genes ($|\text{fold change}| \geq 2$; $P < .05$) in The Cancer Genome Atlas pancreatic cancer tissues with ZIP4 high vs ZIP4 low expression. These data suggested that AKT is an important downstream target of this ZIP4 signaling axis in pancreatic cancer as well (Supplementary Figure 5*H*). Consistently, the level of phosphorylated AKT, a downstream target of PHLPP2, was reduced in the ZIP4 knockout pancreatic cancer cells (Figure 4*I*, Supplementary Figure 5*I*). Expression of PHLPP2 was also confirmed to be negatively correlated with ZIP4 in human pancreatic cancer tissues by means of IHC staining (Figure 4*J*). These results demonstrated that ZIP4 regulates expression of PHLPP2 through miR-373 in pancreatic cancer.

CircANAPC7 Is Involved in ZIP4-Mediated CREB–miR-373–PHLPP2 Feed-Forward Loop and Inhibits Cell Proliferation in Pancreatic Cancer

To identify the role of circANAPC7 in the ZIP4-mediated malignant phenotype in pancreatic cancer, we performed rescue experiments. Cell viability and colony-formation

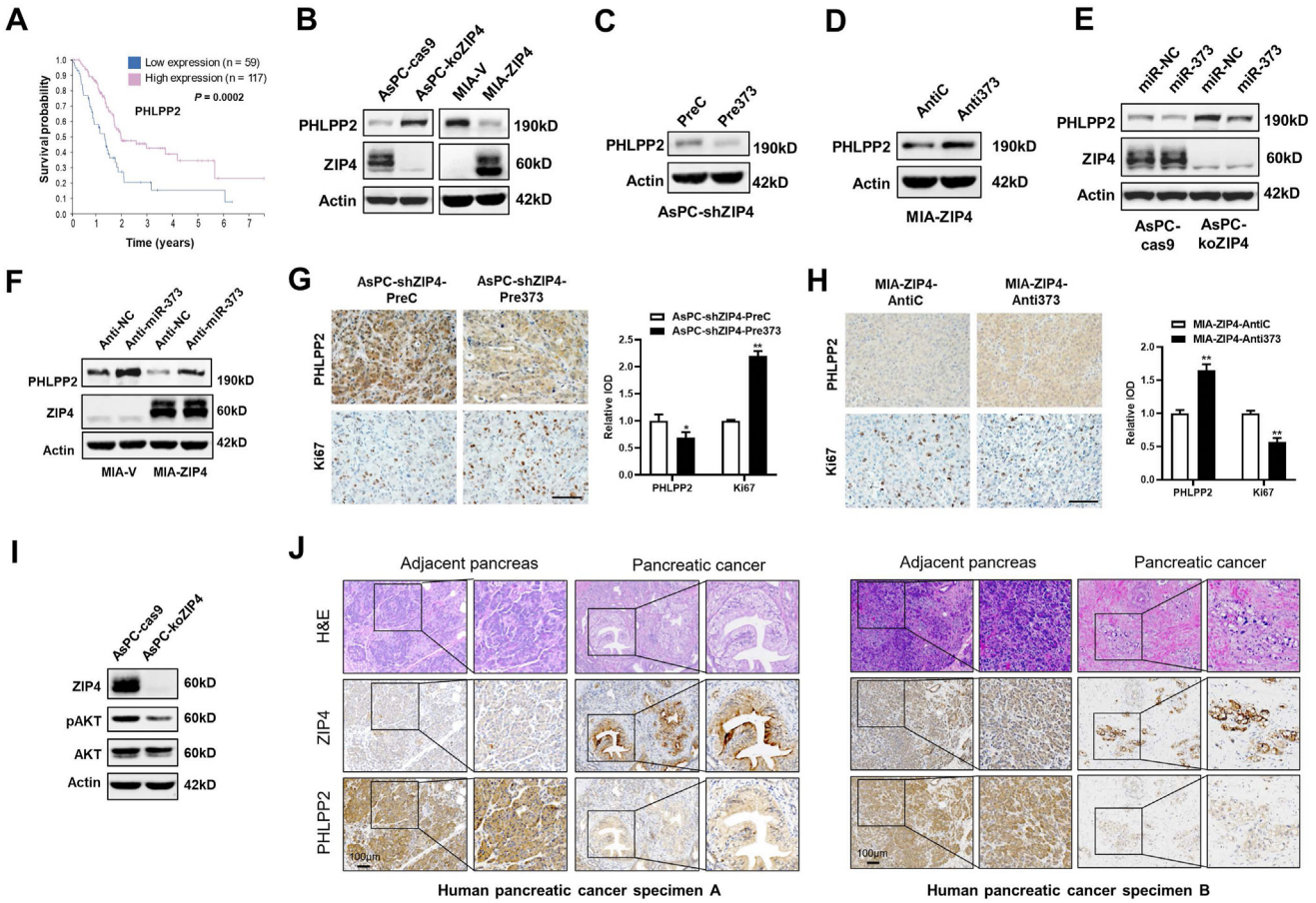

Figure 4. ZIP4 inhibits PHLPP2 expression by increasing the miR-373 level in pancreatic cancer. (*A*) Kaplan-Meier curve for overall survival of patients (n = 176) with pancreatic cancer with low vs high expression of PHLPP2 from The Cancer Genome Atlas database. (*B*) Protein levels of PHLPP2 and ZIP4 in AsPC-cas9/koZIP4, MIA-V/ZIP4 cells. (*C*) Protein levels of PHLPP2 in AsPC-shZIP4-PreC/Pre373 cells. (*D*) Protein levels of PHLPP2 in MIA-ZIP4-anti-C/anti-373 cells. (*E*) Protein levels of PHLPP2 in AsPC-cas9/koZIP4 cells transfected with either miR-NC or miR-373. (*F*) Protein levels of PHLPP2 and ZIP4 in MIA-V/ZIP4 cells transfected with either anti-NC or anti-373. (*G*, *H*) PHLPP2 and Ki67 expression in orthotopic models implanted with AsPC-shZIP4-PreC/Pre373 cells and MIA-ZIP4-anti-C/anti-373 cells. *Scale bar:* 50 μm. (*I*) Protein levels of ZIP4, pAKT, and total AKT in AsPC-cas9/koZIP4 cells. (*J*) Representative H&E and IHC staining images of ZIP4 and PHLPP2 in human pancreatic cancer and cancer-adjacent pancreas tissues. $^{*}P < .05$; $^{**}P < .01$.

assays showed that the increased cell proliferation and colony formation mediated by ZIP4 was reversed by wild-type circANAPC7 overexpression, but not the mutant circANAPC7 (Figure 5*A* and *B*). DNA synthesis assay revealed that wild-type circANAPC7 overexpression, but not the mutant circANAPC7, reversed ZIP4-mediated cell proliferation (Supplementary Figure 6*A*). Subsequently, we used MIA-ZIP4 and AsPC-shZIP4-Pre373 cells with stable overexpression of circANAPC7 to investigate the impact of circANAPC7 in vivo. CircANAPC7 overexpression in both AsPC-shZIP4-Pre373 and MIA-ZIP4 cells significantly inhibited tumor growth in an orthotopic xenograft mouse model (Figure 5*C* and *D*). Because cyclin D1 plays a central role in regulating cell proliferation, and our previous study showed that cyclin D1 is an important downstream target of ZIP4 in pancreatic cancer,[28] therefore, we investigated whether circANAPC7 regulates cell proliferation through cyclin D1 in vitro and in vivo. CircANAPC7 decreased mRNA and protein levels of cyclin D1 in pancreatic cancer cells and mouse xenografts (Supplementary Figure 6*B* and Figure 5*E* and *F*). ZIP4 knockdown down-regulated cyclin D1, while ZIP4 overexpression up-regulated cyclin D1 (Supplementary Figure 6*C*). Moreover, miR-373 blocking could also down-regulate cyclin D1 in vitro (Supplementary Figure 6*D*). These results indicate that circANAPC7 is involved in ZIP4/miR-373–mediated cell proliferation through cyclin D1.

The IHC staining revealed significantly reduced Ki67 level in the circANAPC7 overexpression xenografts (Figure 5*G* and *H*). Furthermore, ZIP4-mediated elevation of phosphorylated AKT level can be reversed by circANAPC7 and PHLPP2 in both 2D and 3D spheroid culture conditions (Figure 5*I* and Supplementary Figure 6*E* and *F*). Because ZIP4 activates miR-373 through transcriptional regulation by increasing phosphorylated CREB and that PHLPP2 is a phosphatase, we examined whether PHLPP2 regulated CREB phosphorylation. We found PHLPP2 silencing increased CREB phosphorylation (Figure 5*J* and

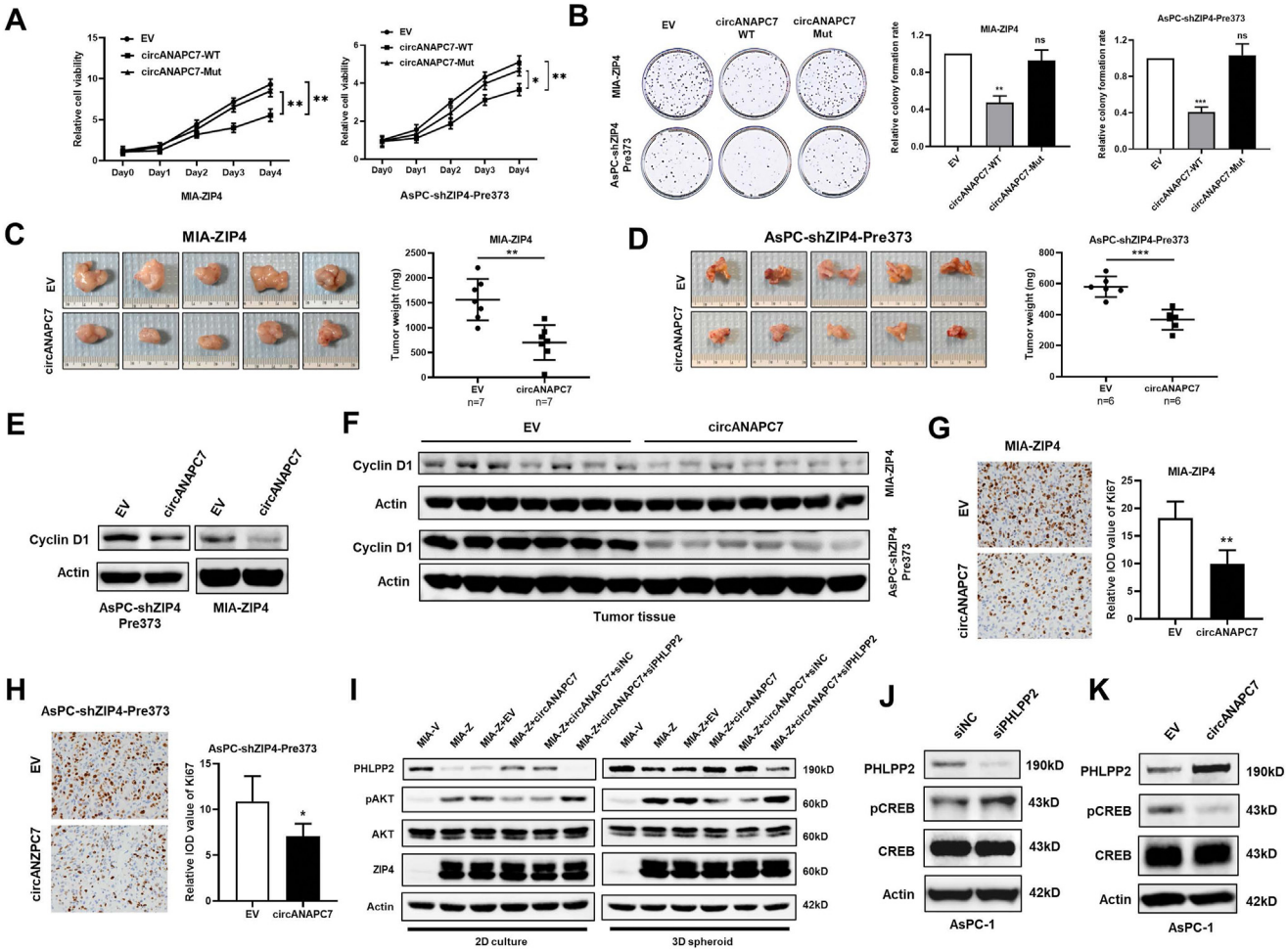

Figure 5. CircANAPC7 suppresses tumor growth in vivo by regulating CREB–miR-373–PHLPP2 feed-forward loop. (*A*) Cell viability of indicated cells was examined by means of MTT assay. (*B*) Colony-formation assay. (*C*) Representative tumor *images* and tumor weight *plot* of MIA-ZIP4-EV/circANAPC7 orthotopic models. (*D*) Representative tumor *images* and tumor weight *plot* of AsPC-shZIP4-Pre373-EV/circANAPC7 orthotopic models. (*E*) Cyclin D1 level was assessed in cell lysates. (*F*) Cyclin D1 level in orthotopic xenografts. (*G, H*) Ki67 IHC staining analysis of orthotopic xenografts. (*I*) Protein levels of PHLPP2, pAKT, and total AKT under 2D and 3D spheroid culture. (*J*, *K*) PHLPP2, pCREB, and total CREB expression was assessed by means of Western blot. ns, not significant; **P* < .05; ***P* < .01; ****P* < .001.

Supplementary Figure 6*G*). Moreover, circANAPC7 overexpression decreased the phosphorylated CREB level in pancreatic cancer cells (Figure 5*K* and Supplementary Figure 6*H*). We also validated that ZIP4 is positively correlated with pCREB and negatively correlated with PHLPP2 in human pancreatic cancer tissues by means of IHC staining (Supplementary Figure 7*A*). These results demonstrated the presence of a feed-forward loop in the ZIP4–CREB–miR-373–PHLPP2 signaling axis, and circANAPC7 inhibits pancreatic cancer cell proliferation through the regulation of this signaling axis.

CircANAPC7 Inhibits ZIP4/miR-373–Mediated Muscle Wasting Through Down- Regulation of Transforming Growth Factor–β

In the cachectic xenograft mouse model, we noticed the body weight of mice implanted with AsPC-shZIP4-Pre373-circANAPC7 cells is significantly higher than the AsPC-shZIP4-Pre373-EV group (Figure 6*A* and *B*). We also examined the body weight of mice injected with MIA PaCa-2 cells, a noncachectic pancreatic cancer cell line, and found that circANAPC7 overexpression cells did not affect murine body weight (Supplementary Figure 7*B*). Cancer-associated body weight loss is mostly due to muscle wasting, we further evaluated muscle wasting in mice implanted with AsPC-shZIP4-Pre373-EV/circANAPC7 cells. At 4 weeks after tumor implantation, the circANAPC7 group showed stronger grip strength compared with the EV group (Figure 6C). In addition, skeletal muscle weight was increased considerably in the AsPC-shZIP4-Pre373-circANAPC7 group compared with the AsPC-shZIP4-Pre373-EV group (Figure 6*D* and *E*). Morphometric analysis of the cross-sectional area of tibialis anterior muscle showed the AsPC-shZIP4-Pre373-circANAPC7 group had a larger cross-sectional area than those in the control group (Figure 6*F*). The increased myofibrillar protein, myosin heavy chain (MyHC), and decreased muscle-specific E3 ubiquitin ligases, Atrogin-1

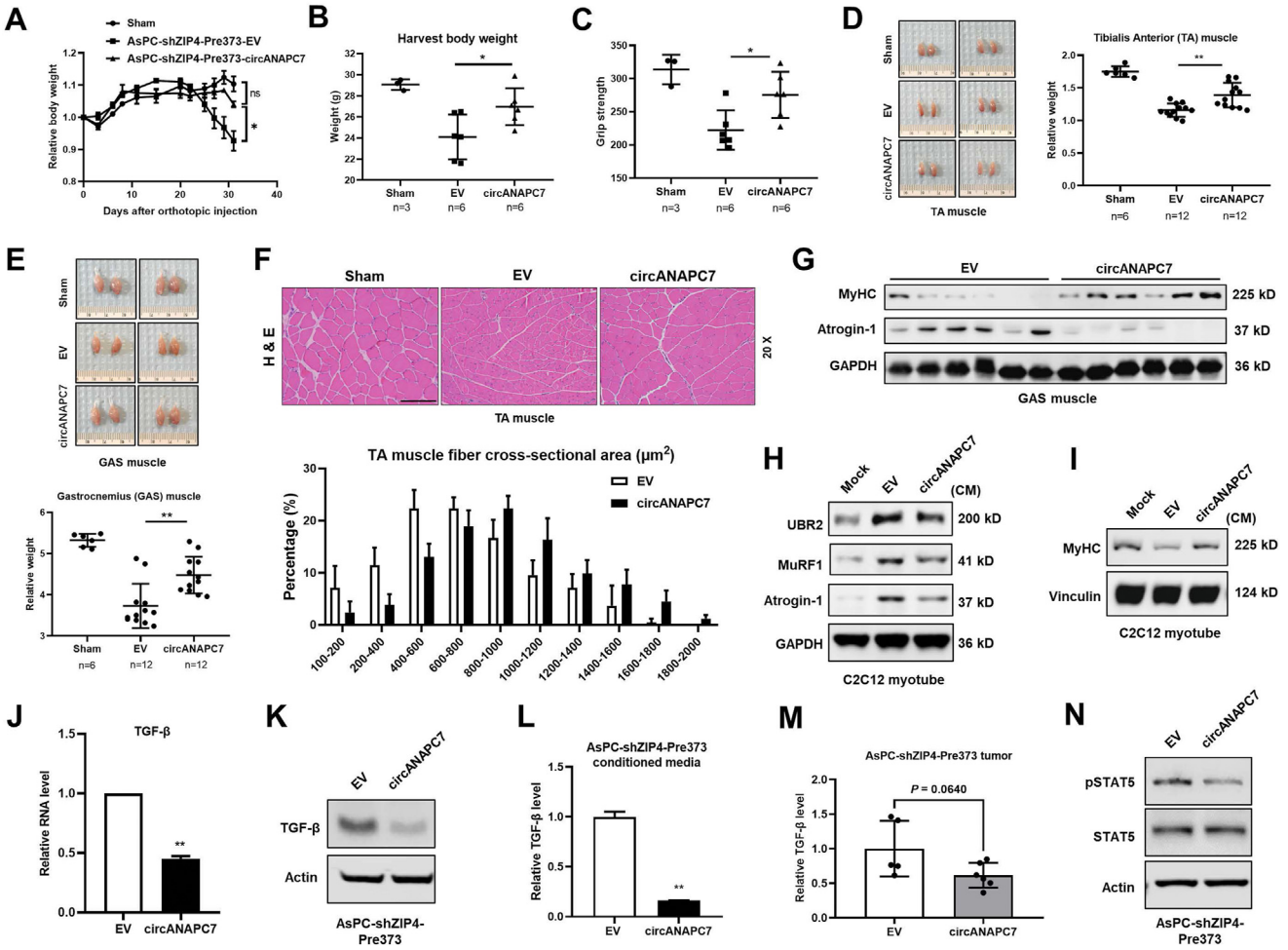

Figure 6. CircANAPC7 inhibits ZIP4/miR-373–mediated muscle wasting in vitro and in vivo. (*A*) Relative body weight curve of mice injected with AsPC-shZIP4-Pre373-EV/circANAPC7 cells. (*B*) Mice body weight. (*C*) Grip strength *plot* of mice. (*D*) Representative *images* of tibialis anterior (TA) muscle and TA muscle weight relative to body weight. (*E*) Representative *images* of gastrocnemius (GAS) muscle and GAS muscle weight relative to body weight. (*F*) Representative *images* of H&E-stained TA muscle sections and quantitative cross-sectional area. (*G*) MyHC and Atrogin-1 protein levels were detected in GAS muscle tissues of mice. (*H*) UBR2, MuRF1, and atrogin-1 levels in C2C12 myotubes cultured in conditioned media for 8 hours. (*I*) MyHC levels in C2C12 myotubes cultured in conditioned media for 72 hours. (*J, K*) mRNA and protein levels of TGF-β in AsPC-shZIP4-Pre373-EV/circANAPC7 cells. (*L*, *M*) TGF-β levels in cell-conditioned media and tumor tissues were detected by enzyme-linked immunosorbent assay. (*N*) STAT5 and pSTAT5 levels were assessed by Western blot.

were also observed in the mice muscle tissues of the AsPC-shZIP4-Pre373-circANAPC7 group (Figure 6*G*). In addition, Kaplan-Meier survival curves showed that circANAPC7 significantly increased median survival of the mice with pancreatic cancer xenografts compared with the control mice, suggesting the role of circANAPC7 in pancreatic cancer growth and cachexia (Supplementary Figure 7*C*). To determine the impact of circANAPC7 on ZIP4-mediated muscle wasting in vitro, we used conditioned media of AsPC-shZIP4-Pre373-EV/circANAPC7 cells to treat C2C12 myotubes and examined the level of muscle atrophy markers and MyHC, the motor protein of muscle thick filaments. The conditioned media from AsPC-shZIP4-Pre373-circANAPC7 cells down-regulated Atrogin-1, MuRF1, and UBR2, but increased MyHC levels (Figure 6*H* and *I*). Conversely, we found conditioned media from miR-373 overexpressed cells up-regulated muscle atrophy markers but decreased MyHC level (Supplementary Figure 7*D* and *E*).

We then examined potential soluble cachectic factors in the context of circANAPC7 mediated anti-cachexia. The multifunctional cytokine TGF-β could activate several pro-cachexia signaling pathways in breast and colon cancer cachexia models and in patients as described previously.[29] We found TGF-β level was significantly decreased in AsPC-shZIP4-Pre373-circANAPC7 group both in the cell lysate and the conditioned media (Figure 6*J–L*). We also observed a reduced level of TGF-β in tumor tissues of mice injected with AsPC-shZIP4-Pre373-circANAPC7 cells, but not MIA-ZIP4-circANAPC7 cells compared with the control group (Figure 6*M* and Supplementary Figure 7*F*). Because STAT5 is a transcriptional regulator mediating AKT induced TGF-β expression and secretion,[30,31] we examined the phosphorylation of STAT5 in pancreatic cancer cells and found AsPC-shZIP4-Pre373-circANAPC7 cells showed reduced STAT5 phosphorylation (Figure 6*N*), which confirmed that STAT5 is the mediator down-regulating TGF-β in AsPC-shZIP4-

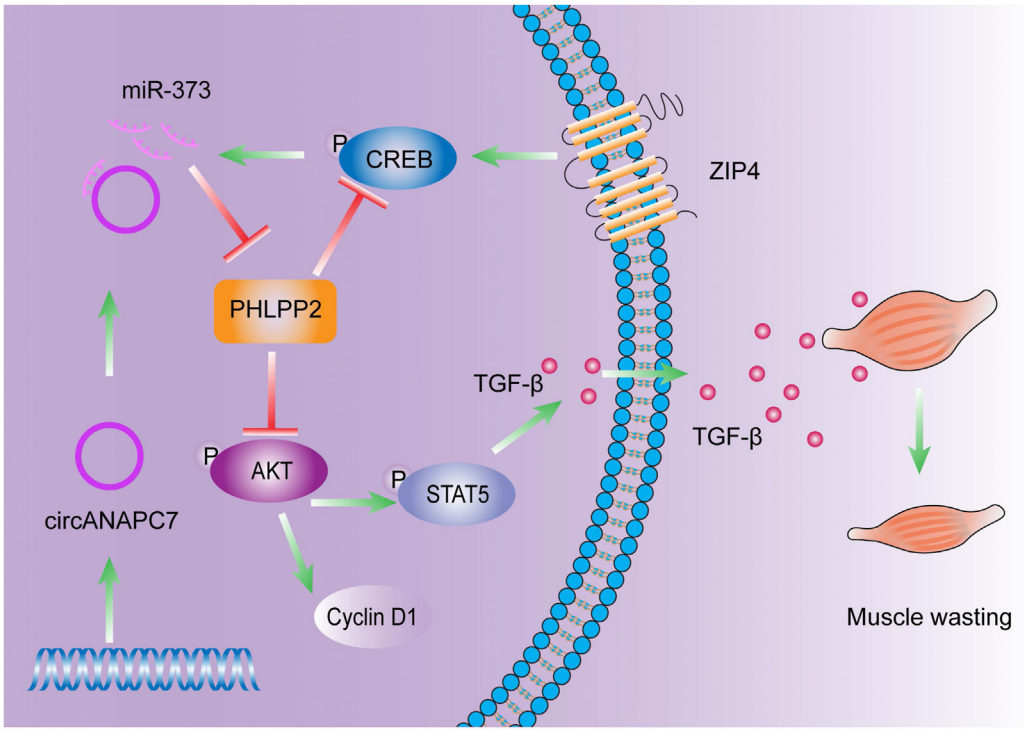

Figure 7. Schematic diagram of circANAPC7 suppressed tumor growth and muscle wasting through PHLPP2–AKT–TGF-β signaling axis in pancreatic cancer. This study identified circANAPC7 as a novel tumor suppressor, which functions through the CREB–miR-373–PHLPP2 axis, leading to AKT dephosphorylation and cyclin D1 and TGF-β down-regulation to suppress tumor progression in pancreatic cancer.

Pre373-circANAPC7 cells. Taken together, these results suggest circANAPC7 inhibited ZIP4/miR-373 mediated muscle wasting in vitro and in vivo, at least partially through STAT5/TGF-β signaling in pancreatic cancer (Figure 7).

Discussion

ZIP4 plays important roles in cell proliferation, metastasis, drug resistance, and cancer-associated cachexia in pancreatic cancer.[9–14,32] These findings prompted us to further investigate the signaling network involved in ZIP4-mediated pancreatic cancer progression. In this study, we found that circANAPC7 inhibited ZIP4-mediated cell proliferation through miR-373–PHLPP2–AKT signaling axis in 2D cultured cancer cell lines, 3D spheroid/organoid model, and an orthotopic xenograft mouse model. In addition, we demonstrated that circANAPC7 inhibited ZIP4-mediated cancer cachexia by inhibiting TGF-β secretion in cancer cells. These findings suggested the involvement of circANAPC7 in ZIP4-mediated pancreatic cancer progression and cachexia, thereby providing a novel therapeutic strategy for pancreatic cancer treatment.

miR-373 is a human embryonic stem cell–specific miRNA and has diverse functions in human cancer.[33] Previously, we found that ZIP4 up-regulated miR-373 by activating CREB, and that miR-373 was responsible for ZIP4-promoted cell proliferation in pancreatic cancer.[10] In this study, we identified PHLPP2 as a novel target of miR-373. We found circANAPC7 serves as a miR-373 sponge, resulting in the increased expression of PHLPP2 and decreased AKT phosphorylation thereby inhibiting pancreatic cancer cell proliferation. Moreover, we found the conditioned media from miR-373 overexpressed cells increased the protein level of muscle atrophy markers in C2C12 myotubes, suggesting miR-373 also plays an important role in cancer cachexia.

Previous studies showed that circRNAs play critical roles in cancer growth, metastasis, stemness, and resistance to therapy.[34,35] Guo et al[20] reported that circBFAR promotes tumor growth and metastasis in pancreatic cancer by up-regulating MET through competitively binding to miR-34b. Chen et al[19] demonstrated that circPTN promotes stemness in glioma by increasing the level of stemness markers (Nestin, CD133, SOX9, and SOX2). Zhang et al[21] reported that circUHRF1 was associated with resistance to anti-PD1 therapy in hepatocellular carcinoma through inhibiting natural killer cell function by increasing TIM-3 level. However, the function of circRNAs in pancreatic cancer muscle wasting and cachexia is largely unknown. Recently, a microarray analysis suggested that circANAPC7 was down-regulated in pancreatic cancer tissues compared with adjacent benign tissues.[26] Here, we systematically evaluated circANAPC7 function in pancreatic cancer progression and cachexia and found that circANAPC7 suppressed pancreatic cancer cell proliferation in 2D and 3D spheroid/organoid conditions. Furthermore, circANAPC7 suppressed cell growth and cancer cachexia in pancreatic cancer cell lines and mouse models. CircRNAs have been reported to play

critical roles in cancer progression; however, little is known about circRNA in muscle wasting and cancer cachexia. We found circANAPC7 reduced the levels of muscle degradation–associated ligases, thus reversed the muscle wasting in cachectic mice. Intriguingly, we also identified circANAPC7 acts as a sponge for miR-373, which serves as the downstream of CREB and upstream of PHLPP2. We further showed that PHLPP2 could dephosphorylate CREB, forming a CREB–miR-373–PHLPP2 feed-forward loop to inhibit pancreatic cancer cell progression.

PHLPP2 is a member of the PHLPP phosphatase family and is known to inhibit cell growth by inhibiting proliferation and promoting apoptosis.[27,32,36,37] Oncogenic kinases AKT, PKC, S6K, and pro-apoptotic kinase Mst1 are functional targets of the PHLPP family.[38] AKT was found to be a downstream target of ZIP4-mediated EMT transition in human nasopharyngeal carcinoma cells, but the underlying mechanism is not clear.[39] In this study, we revealed the ZIP4-dependent regulation of AKT is mediated by PHLPP2. CircANAPC7 inhibits pancreatic cancer cell proliferation by reducing the AKT phosphorylation through regulating PHLPP2 expression. Moreover, we found PHLPP2 could regulate CREB phosphorylation, forming a CREB–miR-373–PHLPP2 feed-forward loop. These results suggest circANAPC7 regulated PHLPP2/AKT is critical for ZIP4/CREB/miR-373 mediated pancreatic cancer cell proliferation and cachexia.

Cancer cachexia usually presents with >5% of body weight loss within 6 months and develops from pre-cachexia to cachexia to refractory cachexia.[4,40] Muscle wasting is a signature event of cancer cachexia, which severely affects patients' mortality because of weakness and fatigue.[41] Increased myofibrillar degradation was observed in skeletal muscle wasting caused by activation of the protein-degradation pathway, including the ubiquitin-proteasome pathway and autophagy-lysosome pathway.[42] The inflammatory factor was considered as a key mediator triggering the activation of the protein-degradation pathway in muscle.[29,43] Currently, very few studies focus on the role of circRNA in cancer cachexia, especially muscle wasting. Zhang et al[44] reported that exosomal circular RNA ciRS-133 derived from gastric tumor promotes browning of white adipose tissue by targeting the miR-133/PRDM16 pathway. Recently, Ding et al[45] demonstrated the role of circPTK2 in promoting lipolysis and reducing adipogenesis. To our knowledge, this study is the first to report the impact of circRNA on skeletal muscle wasting and cachexia of pancreatic cancer. We found the overexpression of circANAPC7 in pancreatic cancer cells relieved muscle wasting in mice, as indicated by increased muscle mass, decreased muscle atrophy proteins (atrogin-1, MuRF1, and UBR2) level, and increased myofibrillar protein (MyHC). Emerging evidence has shown that TGF-β plays critical roles in cancer-associated cachexia, including muscle wasting and adipose loss.[29,43] We found that circANAPC7 up-regulates PHLPP2, leading to dephosphorylation of AKT and CREB. TGF-β blockade reduced the metabolic changes of pancreatic cancer cachexia and improved overall survival.[46] Consistent with previous study,[30] our results showed that circANAPC7 decreased TGF-β by dephosphorylating STAT5. These results suggest that circANAPC7 could effectively ameliorate muscle wasting of pancreatic cancer via PHLPP2–AKT–STAT5–TGF-β signaling axis.

In conclusion, our current study demonstrated that circANAPC7 inhibits ZIP4-mediated cell proliferation by serving as a miR-373 sponge to increase PHLPP2 levels, which in turn results in decreased AKT phosphorylation and cyclin D1 expression. CircANAPC7 also inhibits ZIP4-mediated cancer cachexia by decreasing TGF-β expression and secretion through regulating the AKT/STAT5 signaling. Our results may provide a novel strategy for pancreatic cancer treatment by ameliorating cancer cachexia.

Supplementary Material

Note: To access the supplementary material accompanying this article, visit the online version of *Gastroenterology* at www.gastrojournal.org, and at http://doi.org/10.1053/j.gastro.2022.02.017.

References

1. Siegel RL, Miller KD, Fuchs HE, et al. Cancer statistics, 2021. CA Cancer J Clin 2021;71:7–33.
2. Mizrahi JD, Surana R, Valle JW, et al. Pancreatic cancer. Lancet 2020;395:2008–2020.
3. Baracos VE, Martin L, Korc M, et al. Cancer-associated cachexia. Nat Rev Dis Primers 2018;4:17105.
4. Fearon K, Strasser F, Anker SD, et al. Definition and classification of cancer cachexia: an international consensus. Lancet Oncol 2011;12:489–495.
5. Petruzzelli M, Wagner EF. Mechanisms of metabolic dysfunction in cancer-associated cachexia. Genes Dev 2016;30:489–501.
6. Bafaro E, Liu Y, Xu Y, et al. The emerging role of zinc transporters in cellular homeostasis and cancer. Signal Transduct Target Ther 2017;2.
7. Yu Z, Yu Z, Chen ZB, et al. Zinc chelator TPEN induces pancreatic cancer cell death through causing oxidative stress and inhibiting cell autophagy. J Cell Physiol 2019;234:20648–20661.
8. **Yang J, Zhang Y**, Cui X, et al. Gene profile identifies zinc transporters differentially expressed in normal human organs and human pancreatic cancer. Curr Mol Med 2013;13:401–409.
9. Li M, Zhang Y, Liu Z, et al. Aberrant expression of zinc transporter ZIP4 (SLC39A4) significantly contributes to human pancreatic cancer pathogenesis and progression. Proc Natl Acad Sci U S A 2007;104:18636–18641.
10. **Zhang Y, Yang J**, Cui X, et al. A novel epigenetic CREB-miR-373 axis mediates ZIP4-induced pancreatic cancer growth. EMBO Mol Med 2013;5:1322–1334.
11. **Liu M, Yang J, Zhang Y**, et al. ZIP4 promotes pancreatic cancer progression by repressing ZO-1 and claudin-1 through a ZEB1-dependent transcriptional mechanism. Clin Cancer Res 2018;24:3186–3196.
12. **Liu M, Zhang Y, Yang J**, et al. ZIP4 increases expression of transcription factor ZEB1 to promote integrin alpha3beta1 signaling and inhibit expression of the

gemcitabine transporter ENT1 in pancreatic cancer cells. Gastroenterology 2020;158:679–692.e1.
13. **Liu M, Zhang Y, Yang J**, et al. Zinc-dependent regulation of ZEB1 and YAP1 coactivation promotes epithelial-mesenchymal transition plasticity and metastasis in pancreatic cancer. Gastroenterology 2021; 160:1771–1783.e1.
14. **Yang J, Zhang Z, Zhang Y**, et al. ZIP4 promotes muscle wasting and cachexia in mice with orthotopic pancreatic tumors by stimulating RAB27B-regulated release of extracellular vesicles from cancer cells. Gastroenterology 2019;156:722–734.e6.
15. Kristensen LS, Andersen MS, Stagsted LVW, et al. The biogenesis, biology and characterization of circular RNAs. Nat Rev Genet 2019;20:675–691.
16. Liu H, Lei C, He Q, et al. Nuclear functions of mammalian MicroRNAs in gene regulation, immunity and cancer. Mol Cancer 2018;17:64.
17. **Zhong YX, Du YJ, Yang X**, et al. Circular RNAs function as ceRNAs to regulate and control human cancer progression. Mol Cancer 2018;17.
18. **Memczak S, Jens M, Elefsinioti A**, et al. Circular RNAs are a large class of animal RNAs with regulatory potency. Nature 2013;495:333–338.
19. Chen J, Chen T, Zhu Y, et al. circPTN sponges miR-145-5p/miR-330-5p to promote proliferation and stemness in glioma. J Exp Clin Cancer Res 2019;38:398.
20. **Guo X, Zhou Q**, Su D, et al. Circular RNA circBFAR promotes the progression of pancreatic ductal adenocarcinoma via the miR-34b-5p/MET/Akt axis. Mol Cancer 2020;19:83.
21. Zhang PF, Gao C, Huang XY, et al. Cancer cell-derived exosomal circUHRF1 induces natural killer cell exhaustion and may cause resistance to anti-PD1 therapy in hepatocellular carcinoma. Mol Cancer 2020; 19:110.
22. Shao F, Huang M, Meng F, et al. Circular RNA signature predicts gemcitabine resistance of pancreatic ductal adenocarcinoma. Front Pharmacol 2018;9:584.
23. Hong OY, Mou LJ, Luk C, et al. Immortal human pancreatic duct epithelial cell lines with near normal genotype and phenotype. Am J Pathol 2000; 157:1623–1631.
24. **Lal A, Thomas MP, Altschuler G**, et al. Capture of microRNA-bound mRNAs identifies the tumor suppressor miR-34a as a regulator of growth factor signaling. PLoS Genet 2011;7:e1002363.
25. Liu M, Wang Q, Shen J, et al. Circbank: a comprehensive database for circRNA with standard nomenclature. RNA Biol 2019;16:899–905.
26. Li H, Hao X, Wang H, et al. Circular RNA expression profile of pancreatic ductal adenocarcinoma revealed by microarray. Cell Physiol Biochem 2016; 40:1334–1344.
27. Brognard J, Sierecki E, Gao T, et al. PHLPP and a second isoform, PHLPP2, differentially attenuate the amplitude of Akt signaling by regulating distinct Akt isoforms. Mol Cell 2007;25:917–931.
28. Zhang Y, Bharadwaj U, Logsdon CD, et al. ZIP4 regulates pancreatic cancer cell growth by activating IL-6/STAT3 pathway through zinc finger transcription factor CREB. Clin Cancer Res 2010;16:1423–1430.
29. Wang G, Biswas AK, Ma WC, et al. Metastatic cancers promote cachexia through ZIP14 upregulation in skeletal muscle. Nat Med 2018;24:770–781.
30. Yang S, Wang J, Brand DD, et al. Role of TNF-TNF receptor 2 signal in regulatory T cells and its therapeutic implications. Front Immunol 2018;9:784.
31. Jones N, Vincent EE, Cronin JG, et al. Akt and STAT5 mediate naive human CD4+ T-cell early metabolic response to TCR stimulation. Nat Commun 2019; 10:2042.
32. Zhang YQ, Chen CY, Yao QZ, et al. ZIP4 upregulates the expression of neuropilin-1, vascular endothelial growth factor, and matrix metalloproteases in pancreatic cancer cell lines and xenografts. Cancer Biol Ther 2010; 9:235–241.
33. **Voorhoeve PM, le Sage C**, Schrier M, et al. A genetic screen implicates miRNA-372 and miRNA-373 as oncogenes in testicular germ cell tumors. Cell 2006; 124:1169–1181.
34. **Zhang Y, Zhang XO**, Chen T, et al. Circular intronic long noncoding RNAs. Mol Cell 2013;51:792–806.
35. Chen LL. The biogenesis and emerging roles of circular RNAs. Nat Rev Mol Cell Biol 2016;17:205–211.
36. Liu J, Eckert MA, Harada BT, et al. m(6)A mRNA methylation regulates AKT activity to promote the proliferation and tumorigenicity of endometrial cancer. Nat Cell Biol 2018;20:1074–1083.
37. Nitsche C, Edderkaoui M, Moore RM, et al. The phosphatase PHLPP1 regulates Akt2, promotes pancreatic cancer cell death, and inhibits tumor formation. Gastroenterology 2012;142:377–387.e1–e5.
38. Yan Y, Krecke KN, Bapat AS, et al. Phosphatase PHLPP2 regulates the cellular response to metabolic stress through AMPK. Cell Death Dis 2021;12:904.
39. **Zeng Q, Liu YM, Liu J**, et al. Inhibition of ZIP4 reverses epithelial-to-mesenchymal transition and enhances the radiosensitivity in human nasopharyngeal carcinoma cells. Cell Death Dis 2019;10:588.
40. Fearon K, Arends J, Baracos V. Understanding the mechanisms and treatment options in cancer cachexia. Nat Rev Clin Oncol 2013;10:90–99.
41. Poulia KA, Sarantis P, Antoniadou D, et al. Pancreatic cancer and cachexia-metabolic mechanisms and novel insights. Nutrients 2020;12.
42. Liu Z, Sin KWT, Ding H, et al. p38beta MAPK mediates ULK1-dependent induction of autophagy in skeletal muscle of tumor-bearing mice. Cell Stress 2018;2:311–324.
43. Guttridge DC. A TGF-beta pathway associated with cancer cachexia. Nat Med 2015;21:1248–1249.
44. **Zhang H, Zhu L**, Bai M, et al. Exosomal circRNA derived from gastric tumor promotes white adipose browning by targeting the miR-133/PRDM16 pathway. Int J Cancer 2019;144:2501–2515.
45. **Ding Z, Sun D, Han J**, et al. Novel noncoding RNA CircPTK2 regulates lipolysis and adipogenesis in cachexia. Mol Metab 2021;53:101310.
46. **Greco SH, Tomkotter L, Vahle AK**, et al. TGF-beta blockade reduces mortality and metabolic changes in a

validated murine model of pancreatic cancer cachexia. PLoS One 2015;10:e0132786.

Author names in bold designate shared co-first authorship.

Received November 2, 2021. Accepted February 9, 2022.

Correspondence
Address correspondence to: Min Li, PhD, Department of Medicine, Department of Surgery, The University of Oklahoma Health Sciences Center, 975 NE 10th Street, BRC 1262A, Oklahoma City, Oklahoma 73104. e-mail: Min-Li@ouhsc.edu.

CRediT Authorship Contributions
Xiuhui Shi, MD, PhD (Conceptualization: Lead; Data curation: Lead; Formal analysis: Lead; Investigation: Lead; Project administration: Lead; Writing – original draft: Lead; Writing – review & editing: Lead).

Jingxuan Yang, PhD (Conceptualization: Equal; Data curation: Equal; Formal analysis: Equal; Methodology: Lead; Project administration: Equal; Supervision: Equal; Validation: Lead; Visualization: Lead; Writing – original draft: Equal; Writing – review & editing: Equal).

Mingyang Liu, MD, PhD (Conceptualization: Equal; Data curation: Equal; Formal analysis: Lead; Investigation: Equal; Validation: Lead; Visualization: Equal; Writing – review & editing: Equal).

Yuqing Zhang, PhD (Conceptualization: Lead; Data curation: Equal; Formal analysis: Equal; Methodology: Lead; Supervision: Equal; Visualization: Equal; Writing – review & editing: Lead).

Zhijun Zhou, MD (Conceptualization: Equal; Data curation: Supporting; Formal analysis: Equal; Investigation: Supporting; Methodology: Equal; Project administration: Equal; Software: Equal; Visualization: Lead; Writing – review & editing: Lead).

Wenyi Luo, MD, PhD (Formal analysis: Equal; Investigation: Supporting; Methodology: Equal; Resources: Equal; Visualization: Supporting; Writing – review & editing: Supporting).

Kar-Ming A. Fung, MD, PhD (Formal analysis: Supporting; Methodology: Equal; Resources: Equal; Visualization: Supporting; Writing – review & editing: Supporting).

Chao Xu, PhD (Formal analysis: Supporting; Methodology: Supporting; Resources: Supporting; Software: Equal; Visualization: Supporting; Writing – review & editing: Equal).

Michael S. Bronze, MD (Resources: Equal; Supervision: Equal; Writing – review & editing: Equal).

Courtney W. Houchen, MD (Resources: Equal; Supervision: Equal; Writing – review & editing: Equal).

Min Li, PhD (Conceptualization: Lead; Funding acquisition: Lead; Resources: Lead; Supervision: Lead; Writing – review & editing: Lead).

Conflicts of interest
The authors disclose no conflicts.

Funding
This work was supported in part by the William and Ella Owens Medical Research Foundation (Min Li), United States; Department of Medicine at University of Oklahoma Health Sciences Center, United States.

Supplementary Materials and Methods

Vector Construction

The human circANAPC7 sequence was amplified from human ANAPC7 transcript and then inserted into pcDNA3.1 (+) circRNA mini vector (#60648; Addgene) using the EcoRV and SacII sites. circANAPC7 sequence and 3′UTR and PHLPP2 were inserted into Dual-Luciferase miRNA Target Expression Vector pmiRGlo (#78132; Addgene) using the NheI and XbaI sites. The mutated vectors were generated by the QuikChange Lightning Site-Directed Mutagenesis Kit (#210518; Agilent Technologies). The primer sequences used were provided in Supplementary Table 2.

Lentiviral Expression and Stable Cell Line Construction

The cancer cells with stable overexpression of circANAPC7 were generated by using lentivirus vector EX-NEG-Lv207 (GeneCopoeia). Purified transfer plasmid or control vector co-transfected with packaging plasmid psPAX2 (#12260; Addgene) and envelope plasmid pCMV-VSV-G (#8454; Addgene) were transfected into 293T cells using Lipofectamine 3000 Transfection Reagent (#L3000015; Invitrogen). Viral supernatant was harvested at 48 hours and 72 hours post transfection and filtered through a 0.45-μm polyethersulfone filter, then used to transduce cells in complete medium with 10 mg/mL of polybrene (#TR-1003-G; Millipore) for 48 hours. Transduced cells were selected by Hygromycin (#10687010; Invitrogen) and for 2 weeks in complete culture medium. Cells were analyzed for circANAPC7 level by means of RT-qPCR.

Database Analysis

DECs were identified (|fold change| >1.2; $P < .05$) in the Gene Expression Omnibus dataset (GSE69362) by R (https://www.r-project.org/) through limma package.[e1] CircRNAs with miR-373 binding sites were predicted through the circBank database.[25] mRNAs with miR-373 binding sites were predicted by TargetScan (http://www.targetscan.org/vert_80/) as well as ENCORI (https://starbase.sysu.edu.cn/) database. The human suppressor genes were from the TSGene database (https://bioinfo.uth.edu/TSGene/). Differentially expressed genes between ZIP4-high and ZIP4-low were identified in the The Cancer Genome Atlas pancreatic adenocarcinoma dataset and then applied to Kyoto Encyclopedia of Genes and Genomes pathway analysis in the ConsensusPathDB database (http://cpdb.molgen.mpg.de/CPDB).

RNA and Genomic DNA Extraction

Messenger RNA and circRNA were extracted using PureLink RNA Mini Kit (#12183025; Invitrogen) and TRIzol Reagent (#15596026; Invitrogen) according to the manufacturer's instruction. MicroRNA were extracted mirVana miRNA Isolation Kit (#AM1561; Invitrogen). The nuclear and cytoplasmic RNA were extracted using PARIS Kit (#AM1921; Life Technologies). Genomic DNA was extracted using lysis buffer and proteinase K solution (#03115836001; Roche).

Sanger Sequencing

To validate the result of PCR, the PCR product was purified by PureLink Quick Gel Extraction and PCR Purification Combo Kit (#K220001; Invitrogen) and Sanger sequencing was performed by Laboratory for Molecular Biology and Cytometry Research of University of Oklahoma Health Sciences Center. The divergent primers were used for the amplification and sequencing. Primers used are listed in Supplementary Table 2.

Colony-Formation Assay

Cells were seeded into 3-cm Petri dish (500 cells per dish) and left for 8 or 12 days until formation of visible colonies. Colonies were washed with phosphate-buffered saline (PBS) and fixed with paraformaldehyde for 20 minutes, then stained with 0.5% crystal violet in ethanol for 20 minutes. After staining, the plates were washed and air-dried, and colony-formation rates were analyzed.

Cell Transfection

Small interfering RNA, miRNA mimics and inhibitors were purchased from Life Technologies. The sequences used are shown in Supplementary Table 2. Lipofectamine RNAiMax (#13778150; Invitrogen) was used for transfecting small RNAs, including small interfering RNAs, miRNA mimics and inhibitors. Lipofectamine 3000 Reagent (#L3000015; Invitrogen) was used for plasmid transfection following the manufacturer's protocol.

Western Blot

Protein samples were loaded on 8% SureCast Gel made by SureCast Gel Handcast Bundle A-Hardware and Reagents kit (#HC1000SR; Invitrogen), then separated and transferred to Odyssey Nitrocellulose Membranes (#P/N926-31092; LI-COR Biosciences) using standard procedures. Membranes were then probed with ZIP4 polyclonal antibody (1:1000, #20625-1-AP; Proteintech), PHLPP2 polyclonal antibody (1:1000, #ab71973; Abcam), Akt (Pan) antibody (1:1000, #4691; CST), phospho-Akt (Ser473) antibody (1:500, #4060; CST), CREB antibody (1:1000, #9197; CST), phospho-CREB (Ser133) antibody (1:500, #9198; CST), atrogin-1 antibody (1:1000, #AP2041; ECM Biosciences), cyclin D1 antibody (1:200, H-295; Santa Cruz Biotechnology), UBR2 (1:1000, NBP1-45243; Novus Biologicals), MyHC antibody (1:1000, MF20; DSHB), TGF-β antibody (1:1000, #3711; CST), phospho-Stat5 (Tyr694) rabbit monoclonal antibody (1:1000, #9359; CST), and Stat5 rabbit monoclonal antibody (1:1000, #25656; CST) at 4°C overnight, and then washed 3 times in Tris-buffered saline with 0.1% Tween 20 and incubated with near-infrared–coupled secondary antibody (1:5000) for 1 hour at room temperature. Western blot signal was imaged with Odyssey Fc Infrared Imaging System (LI-COR Biosciences).

Immunohistochemical Staining

Collected tissues were fixed in 4% paraformaldehyde and then embedded and sectioned by the pathology core of University of Oklahoma Health Sciences Center. Deparaffinize paraffin slides in Xylene 2 times, 5 minutes each, then hydrate slides in 100%, 90%, 70%, 50% ethanol, 1 minute each. Wash in distilled water for 5 minutes. Perform antigen unmasking using a citrate-based antigen unmasking solution (#H-3300; Vector Laboratories). Incubating the sections in 3% H_2O_2 for 10 minutes to quench endogenous peroxidase activity. Wash in PBS for 5 minutes. Incubate sections for 20 minutes with 2.5% normal horse serum (#MP-7401; Vector Laboratories). Incubate with primary antibody diluted in normal horse serum at 4°C overnight. Wash in PBS for 5 minutes. Incubate for 30 minutes with ImmPRESS Horse Anti-Rabbit IgG Polymer Reagent (#MP-7401; Vector Laboratories). Wash in PBS for 5 minutes. Incubate in 3,3′-Diaminobenzidine tetra hydrochloride peroxidase substrate solution (#SK-4105; Vector Laboratories) develops from 30 seconds to 1 minute. Rinse sections in tap water. Counterstain slides by incubating sections with hematoxylin QS (#H-3404; Vector Laboratories) for 5 seconds. Rinse sections with running tap water until rinse water is colorless. Go through dehydration process with 50%, 70%, 80%, 90%, and 100%, 1 minute each, then 2 times Xylene, 2 minutes each. Mount sections with Xylene-based mounting medium (#C573; O. Kinder). Stained slides were assessed using microscope (Olympus). PHLPP2 and Ki67 staining were analyzed by Image-Pro Plus 6.0 (Media Cybernetics). Cross-sectional areas of H&E-stained TA muscle sections were quantified by using Image J software (National Institutes of Health).

Protein Extraction

Cells were lysed by cOmplete Lysis-M (#04719956001; Roche) supplemented with protease inhibitor (#04693116001; Roche) and phosphatase inhibitor (#04906837001; Roche) for 5 minutes. Centrifuge the tubes at 12,000 rpm for 10 minutes at 4°C. Collect the supernatant in fresh tubes and place on ice. Protein concentrations of cell lysates were measured with Pierce BCA Protein Assay Kit (Thermo Scientific; #23225). Cell lysates were heated at 80°C for 10 minutes mixed with 1X NuPAGE LDS Sample Buffer (#NP0008; Invitrogen) and NuPAGE Sample Reducing Agent (#NP0009; Invitrogen).

Reverse Transcription Quantitative Real-Time Polymerase Chain Reaction

Messenger RNA and circRNA were reverse transcribed using High-Capacity cDNA Reverse Transcription Kit (#4368813; Applied Biosystems). MicroRNA was reverse transcribed using QuantiMir Kit (#RA420A-1; System Biosciences). FastStart Taq DNA Polymerase (#04738381001, Roche) was used for PCR. Power SYBR Green PCR Master Mix (#4367659; Applied Biosystems) was used for RT-qPCR. The complementary DNA and genomic DNA PCR products were detected using agarose (#A6013; Sigma-Aldrich) gel electrophoresis. The circRNA and mRNA levels were normalized to ACTB or GAPDH. The miRNA level was normalized to U6 small nuclear RNA. Relative RNA expression levels were analyzed by the $2^{-\Delta\Delta Ct}$ method. Primers were listed in Supplementary Table 2.

MTT Assay

The viability of cancer cells was detected by MTT kit; 3000–5000 cells in 100 μL 10% fetal bovine serum medium were incubated in quintuplicate in 96-well plates. At days 0, 1, 2, 3, and 4, the MTT reagent in medium was added to each well and incubated for 2 hours at 37°C. The optical density at 560/590 nm was measured using a microplate reader (Synergy H1; BioTek).

5-Ethynyl-2′-Deoxyuridine Assay

The DNA synthesis assay was detected by 5-ethynyl-2′-deoxyuridine (EdU) assay using Click-iT EdU Cell Proliferation Kit for Imaging, Alexa Fluor 594 dye (#C10339; Invitrogen). Cells were seeded in the Nunc Lab-Tek Chamber slide (#154526; Thermo Scientific) at the desired density overnight. Cells were added with 10 μM EdU in complete medium and incubated for 1–2 hours at 37°C. Cells were then fixed with 3.7% formaldehyde solution (#F8775; Sigma-Aldrich) and permeabilization with 0.5% Triton X-100 (#T8787; Sigma-Aldrich), followed by EdU detection using Click-iT reaction cocktail. Cell nuclei were stained with Hoechst 33342. Images were taken using a fluorescence microscope (Olympus) and cell proliferation rate was calculated according to the manufacturer's instructions.

Enzyme-Linked Immunosorbent Assay

Quantification of TGF-β in cell-conditioned medium and tumor tissues were analyzed by enzyme-linked immunosorbent assay (ELISA) following the manufacturer's instruction (Human TGF-β ELISA Kit, #BMS249-4; Invitrogen). Briefly, TGF-β release from cancer cells were analyzed by ELISA in various cell-conditioned media after 72 hours of culture. TGF-β levels in tumor tissues were analyzed by ELISA from orthotopic xenografts of nude mice on day 31, and the results were normalized to total protein concentration examined by BCA assay. Samples were diluted with assay buffer and added to precoated microwells with anti-human TGF-β antibody, followed by incubating with biotin-conjugated capture antibody, streptavidin-horseradish peroxidase, and substrate. Detection was achieved by evaluating the conjugated enzyme activity via reading absorbance of microwell at 450 nm wavelength and wavelength correction at 620 nm.

Supplementary Reference

e1. Ritchie ME, Phipson B, Wu D, et al. limma powers differential expression analyses for RNA-sequencing and microarray studies. Nucleic Acids Res 2015;43:e47.